Rotaxanes Incorporating Two Different Coordinating Units in Their Thread: Synthesis and Electrochemically and Photochemically Induced Molecular Motions

Nicola Armaroli,*,‡ Vincenzo Balzani,*,§ Jean-Paul Collin,† Pablo Gaviña,†,⊥ Jean-Pierre Sauvage,*,† and Barbara Ventura§

Contribution from the Laboratoire de Chimie Organo-Minérale, UMR du CNRS no. 7513, 4, rue Blaise Pascal, Faculté de Chimie, Université Louis Pasteur, 67070 Strasbourg Cedex, France, Istituto di Fotochimica e Radiazioni d'Alta Energia del CNR, Via Gobetti 101, 40129 Bologna, Italy, and Dipartimento di Chimica "G. Ciamician", Università di Bologna, Via Selmi 2, 40126 Bologna, Italy

Received November 23, 1998

Abstract: Three different multicomponent molecular systems have been synthesized by means of the three-dimensional template effect of copper(I). These systems incorporate both a coordinating ring (2,9-diphenyl-1,10-phenanthroline-containing 30-membered ring) and a molecular string which consists of two different coordination sites (2,9-disubstituted-1,10-phenanthroline and 5,5″-disubstituted-2,2′:6′,2″-terpyridine unit). Each end of the string could be functionnalyzed by a small group or by a bulky stopper (tris(*p-tert*-butylphenyl)-(4-hydroxyphenyl)methane), leading to an unstoppered compound, to a semi-rotaxane, or to a real rotaxane. As in the case of a disymmetrical copper [2]-catenane, large reversible molecular motions have been induced both electrochemically and photochemically. The driving force of the rearrangement processes is the high stability of two markedly different coordination environments for the copper(I) and copper(II) ions. In the copper(I) state, two phenanthroline units (one of the ring, one of the string) interact with the metal ion in a tetrahedral geometry ($Cu^{I}_{(4)}$), whereas in the copper(II) state, one phenanthroline belonging to the ring and the terpyridine of the string afford a five-coordinate geometry ($Cu^{II}_{(5)}$). The rates of the molecular motion processes (from $Cu^{II}_{(4)}$ to $Cu^{II}_{(5)}$ and from $Cu^{I}_{(5)}$ to $Cu^{I}_{(4)}$) are respectively faster and slower (minutes time scale) as compared to those for the catenane species. This result could be interpreted on the basis of structural differences between the rotaxane and catenane systems.

Introduction

In biology, many "molecular motors" or "machines" play an essential role. These systems are multicomponent assemblies undergoing large-amplitude geometrical changes or leading to the locomotion of one of the components, under the action of either an external stimulus (pH change, redox process, light pulse, etc.) or a chemical gradient. Many examples are known of proteins which undergo important shape modifications (folding−defolding) after a signal has been sent to the protein.[1] Real molecular motors consist of several units, among which some parts will be considered as motionless and some others will move continuously while a "fuel" is "burned", which translates, in biological systems, as: ATP is hydrolyzed. Linear motors such as myosin[2] (from skeletal muscle) or kinesin[3] (from brain) have been known for many years, and knowledge about them has made considerable progress recently. By contrast, few rotary motors have been identified and investigated.[4] The most spectacular example is that of ATPase, whose rotation motion was postulated long ago[5] but which could be directly observed only recently.[6] ATPase consists of a "stator", with six proteins ($\alpha_3\beta_3$) assembled to form an orange-like unit, a seventh, rodlike, protein (γ) being threaded in the hollow part of the $\alpha_3\beta_3$ unit to form the "rotor". The γ subunit rotates inside the $\alpha_3\beta_3$ assembly with concomitant hydrolysis of ATP or during ATP synthesis when a pH gradient is present.

Threaded or interlocking rings are ideally suited to the construction of fully artificial molecular motors.[7] If a ring is threaded onto a rod, it can either rotate around the axle or undergo a translation movement. Similarly, in catenanes (i.e., interlocking ring multicomponent systems), a ring can glide at will and spin within another ring. Several examples of such compounds have been elaborated and studied in recent years, using threaded and interlocked molecules based on either

* Authors to whom correspondence should be addressed.
† Université Louis Pasteur.
‡ Istituto di Fotochimica e Radiazioni d'Alta Energia del CNR.
§ Università di Bologna.
⊥ Present address: Departament de Quimica Orgànica, Universitat de València, Facultat de Farmàcia, Av. Vicent Andrés Estellés s/n, 16100 Burjassot (València), Spain.

(1) Schenck, H. L.; Dada, G. P.; Gellman S. H. *J. Am. Chem. Soc.* **1996**, *118*, 12487−12494. Dado, G. P.; Gellman S. H. *J. Am. Chem. Soc.* **1993**, *115*, 12609−12610. Bixler, J.; Bakker, G.; McLendon, G. *J. Am. Chem. Soc.* **1992**, *114*, 6938−6939. Thirumalai, D.; Woodson, S. A. *Acc. Chem. Res.* **1996**, *29*, 433−439. Pascher, T.; Chesick, J. P. Winkler, J. R.; Gray H. B. *Science* **1996**, *271*, 1558−1560. Jones C. M.; Henry, E. R.; Hu, Y.; Chan, C.-K.; Luck, S. D.; Bhuyan, A.; Roder, H.; Hofrichter, J.; Eaton W. A. *Proc. Natl. Acad. Sci. U.S.A.* **1993**, *90*, 11860−11864.

(2) Finer, J. T.; Simmons, R. M.; Spudlich, J. A. *Nature* **1994**, *368*, 113−119. Whittaker M.; Wilson-Kubalek, E. M.; Milligan, R. A.; Sweeney, H. L. *Nature* **1995**, *378*, 748−751

(3) Sablin, E. P.; Kull F. J.; Cooke, R.; Vale, R. D.; Fletterick, R. J. *Nature* **1996**, *380*, 555−559. Meyhöfer, E.; Howard, J. *Proc. Natl. Acad. Sci. U.S.A.* **1995**, *92*, 574−578.

(4) Elston, T.; Wang, H.; Oster, G. *Nature* **1998**, *391*, 510−513.

(5) Duncan, T. M.; Bulygin, V. V.; Zhan, Y.; Hutchean, M. L.; Cross, R. L. *Proc. Natl. Acad. Sci. U.S.A.* **1995**, *92*, 10964−10968. Walker, J. E. *Angew. Chem., Int. Ed. Engl.* **1998**, *37*, 2308−2319 and references therein.

(6) Noji, H.; Yasuda, R.; Yoshida, M.; Kinosita, K., Jr. *Nature* **1997**, *386*, 299−302.

(7) Balzani, V.; Gomez-Lopez, M.; Stoddart, J. F. *Acc. Chem. Res.* **1998**, *31*, 1, 405−414. Sauvage, J.-P. *Acc. Chem. Res.* **1998**, *31*, 611−619.

10.1021/ja984051w CCC: $18.00
Published on Web 04/24/1999

acceptor−donor and hydrogen-bonded complexes[8] or transition metal complexes.[9] In the purely organic systems, interesting processes have been evidenced, such as dethreading of an acyclic component from a ring under the action of light[10] or translation of a ring between two distinct positions of a thread, induced by a redox signal.[11]

The present system deals with copper complexes of rotaxane-related compounds, i.e., a ring threaded on a molecular string, both constitutive units being assembled via coordination to the same metal center. Preliminary reports on the synthesis[12] or the electrochemical behavior[13] of the compounds have been published recently.

Results and Discussion

General Principle and Design of the Molecules. Coordination compounds are particularly attractive as components of molecular machines whose motions are driven by an electrochemical signal. Since the stereoelectronic requirements of a metal center can be strongly modified by changing its oxidation state, redox-active transition metal complexes are expected to undergo electrochemically induced rearrangement of the metal coordination sphere. This is particularly true for copper complexes: Cu(I) is usually low-coordinate (coordination number CN $\leq$ 4), whereas Cu(II) is preferably square planar or higher coordinate (CN = 5 or 6). In the molecular machines previously made and investigated in our group, the same general principle is utilized: by reducing or oxidizing the copper center, from a situation corresponding to a stable complex, the system is set out of equilibrium. The relaxation process of the compound implies a large-amplitude motion which will bring the system to its new equilibrium position. In previous work on catenanes, we studied the gliding motion of a ring within the other by setting in motion either one cycle or both rings.[9,14] In the rotaxanes decribed in the present paper, a ring is translated along a rodlike component on which it is threaded (Chart 1).

Chart 1

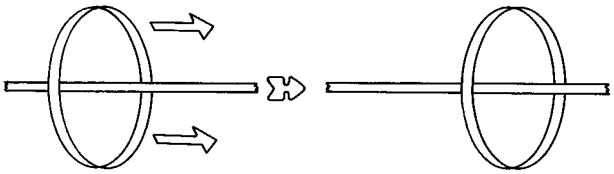

The ring incorporates a bidentate chelate, and the string contains both a bidentate coordinating unit and a terdentate fragment, the string being threaded through the ring via coordination of both components to the same metal center. The system can be switched from four-coordinate (low oxidation state) to five-coordinate (high oxidation state) and vice versa by oxidizing or reducing the transition metal, as represented in Figure 1.

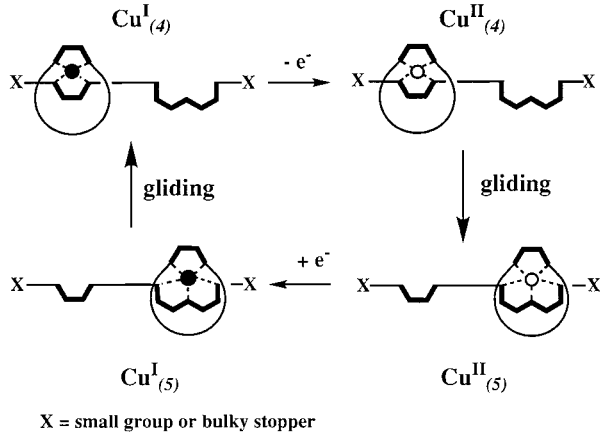

Figure 1. Square scheme in the threaded compounds $\mathbf{18}^+$, $\mathbf{19}^+$, or $\mathbf{24}^+$. The subscripts 4 and 5 indicate the copper coordination number in each complex. The stable $Cu^{I}_{(4)}$ complex is oxidized to an intermediate tetrahedral divalent species, $Cu^{II}_{(4)}$, which undergoes a rearrangement to afford the stable $Cu^{II}_{(5)}$ complex. Upon reduction, a $Cu^{I}_{(5)}$ species is formed as a transient, which finally reorganizes to regenerate the starting complex. The black circle represents Cu(I), and the white circle represents Cu(II).

Synthesis of the Threaded Compounds. The target copper(I) rotaxane and its nonstoppered or partially stoppered analogues are shown in Chart 2.

Chart 2

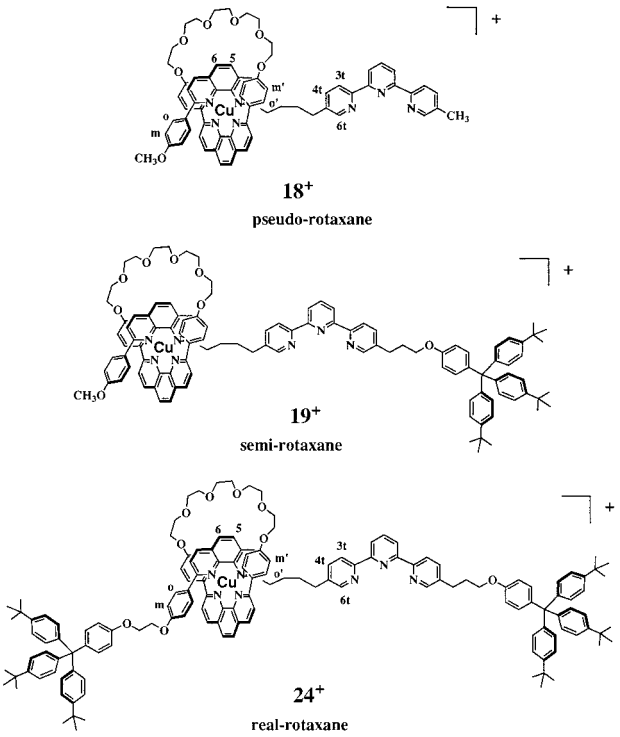

The tetraarylmethane derivative used as stopper group was selected because of its size (no possible threading through the 30-membered ring used as cyclic component) and for its relative ease of access. The synthetic strategy is based on a transition

(8) Ashton, P. R.; Ballardini, R.; Balzani, V.; Boyd, S. E.; Credi, A.; Gandolfi, M. T.; Gomez-Lopez, M.; Iqbal, S.; Philp, D.; Preece, J. A.; Prodi, L.; Ricketts, H.; Stoddart, J. F.; Tolley, M. S.; Venturi, M.; White, A. J. P.; Williams, D. J. *Chem. Eur. J.* **1997**, *3*, 152. Philp, D.; Stoddart, J.-F. *Angew. Chem., Int. Ed. Engl.* **1996**, *35*, 1154−1196. Ashton, P. R.; Ballardini, R.; Balzani, V.; Credi, A.; Gandolfi, M. T.; Menzer, S.; Pérez-Garcia, L.; Prodi, L.; Stoddart, J. F.; Venturi, M.; White, A. J. P.; Williams, D. J. *J. Am. Chem. Soc.* **1995**, *117*, 11171−11197. Credi, A.; Balzani, V.; Longford, S. J.; Stoddart, J. F. *J. Am. Chem. Soc.* **1997**, *119*, 2679−2681.

(9) Livoreil, A.; Dietrich-Buchecker, C. O.; Sauvage, J.-P. *J. Am. Chem. Soc.* **1994**, *116*, 9399−9400. Baumann, F.; Livoreil, A.; Kaim, W.; Sauvage, J.-P. *Chem. Commun.* **1997**, 35−36. Livoreil, A.; Sauvage, J.-P.; Armaroli, N.; Balzani, V.; Flamigni, L.; Ventura, B. *J. Am. Chem. Soc.* **1997**, *119*, 12114−12124.

(10) Ballardini, R.; Balzani, V.; Gandolfi, M. T.; Prodi, L.; Venturi, M.; Philp, D.; Ricketts, H. G.; Stoddart, J. F. *Angew. Chem., Int. Ed. Engl.* **1993**, *32*, 1301−1303.

(11) Bissell, R. A., Córdova, E.; Kaifer, A. E.; Stoddart J. F. *Nature* **1994**, *369*, 133.

(12) Gaviña, P.; Sauvage, J.-P. *Tetrahedron Lett.* **1997**, *38*, 3521−3524.

(13) Collin, J.-P.; Gaviña, P.; Sauvage, J.-P. *J. Chem. Soc., Chem. Commun.* **1996**, 2005−2006. Collin, J.-P.; Gaviña, P.; Sauvage, J.-P. *New J. Chem.* **1997**, *21*, 525−528.

(14) Cárdenas, D. J.; Livoreil, A.; Sauvage, J.-P. *J. Am. Chem. Soc.* **1996**, *118*, 11980−11981.

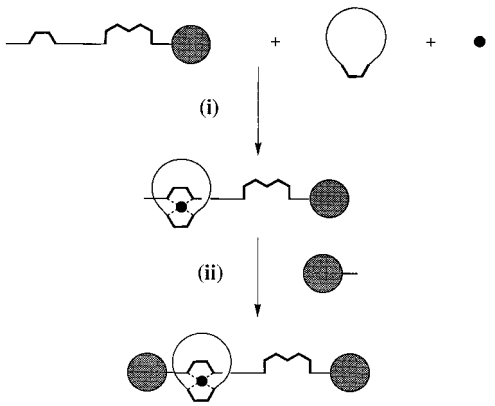

Figure 2. Construction principle: the bidentate chelate (phen, represented by an inverted U) and the terdentate unit (terpy, represented by a stylized M) have been incorporated in an acyclic ligand already bearing a bulky stopper at one end. The ring contains a phen nucleus. (i) In the threading step, copper(I) (represented by a black circle) forces the string to pass through the ring. Since copper(I) has a strong tendency to be four-coordinate, the threading reaction will selectively lead to the precursor represented. (ii) The blocking reaction will be done by attaching a voluminous group at the second end of the coordinating string.

metal-directed process which has been used in our group extensively to make various catenanes and rotaxanes, as depicted in Figure 2. The starting compounds and the intermediate molecules are represented in Figure 3.

Our first approach toward threaded linear systems displaying electrochemically induced molecular motions involved the synthesis of the most simple system: pseudorotaxane **18**$^+$, whose ring incorporates a 2,9-diphenyl-1,10-phenanthroline moiety and whose open-chain molecular string contains two different coordination sites: a 2,9-disubstituted 1,10-phenanthroline (phen) bidentate chelate and a terdentate ligand, 2,2′,6′,2″-terpyridine (terpy), covalently linked by a four-carbon aliphatic chain. Copper(I) was used as a gathering and templating metal center, forcing the string to thread through the coordinating ring while generating a bis-chelate complex between the metal ion and the two phen moieties.

The starting 5,5″-dimethyl-2,2′:6′,2″-terpyridine **1** was prepared from 2-acetyl-5-picoline by Jameson's method[15] or, alternatively, from 2-bromo-5-picoline and 2,6-dibromopyridine following the Stille cross-coupling reaction.[16] **1** was deprotonated with LDA in THF, giving a deep purple compound which was reacted with 1 equiv of THP-protected bromoethanol (THP = tetrahydropyran-2-yl) to afford the monosubstituted derivative **2** in 44% yield. Hydrolysis of the acetal with a catalytic amount of concentrated HCl in refluxing EtOH led to an 85% yield of free alcohol **3**, which was converted first to the mesylate **4** in 95% yield by reaction with mesyl chloride (MsCl) and NEt_3 in CH_2Cl_2 and then to the bromo derivative **5** (97%) by reaction with anhydrous LiBr in refluxing acetone. Separately, the bidentate coordinating unit 2-methyl-9-(*p*-anisyl)-1,10-phenanthroline **13** was prepared from 1,10-phenanthroline as previously reported.[17] Deprotonation of **13** with LDA in THF, followed by reaction with **5** at room temperature, afforded the target bifunctional ligand **14** in 56% yield after workup and column chromatography, as a yellow solid.

The 30-membered macrocycle **17**[18] was chosen as the coordinating ring. The reaction between **17** and $Cu(MeCN)_4BF_4$ in CH_2Cl_2−MeCN under Ar at room temperature led to an orange solution of Cu(**17**)$(MeCN)_2^+$, which was reacted with a CH_2Cl_2 solution of **14** to give the desired pseudorotaxane **18**$^+$ in 75% yield after column chromatography as a brown-red solid. The reaction proceeded regioselectively on the phenanthroline ligand of the string, as was unambiguously shown by ^{1}H NMR and UV−vis spectroscopies. The ^{1}H NMR spectrum of **18**$^+$ shows the typical upfield shifts of the aromatic protons of the phenoxy moieties due to the ring current effect of the 1,10-phenanthroline nuclei, consistent with two phenanthroline units intertwined around a copper(I) center[19] (5.95 and 5.88 ppm for the H_m and $H_{m'}$ and 7.31 and 7.14 for H_o and $H_{o'}$). The absorption at 442 nm in the visible spectrum is typical of these bis(phen) complexes.[19] FAB-MS confirmed the structure, showing an intense peak at *m*/*z* 1216.4 corresponding to the loss of the counterion. The main peak, at *m*/*z* 650.2, corresponds to the loss of the counterion and the macrocycle.

Semi-Rotaxane 19$^+$ and Rotaxane 24$^+$. The main drawback of compound **18**$^+$ is clearly related to the possibility of undergoing a dethreading process, in either the monovalent or the divalent state, leading to chemical irreversibility of the redox-induced motions. An obvious improvement is to covalently attach one or two stoppers at the ends of the thread to afford a semi-rotaxane or a rotaxane, respectively. The chosen blocking group was tris(*p*-*tert*-butylphenyl)(4-hydroxyphenyl)methane since it is large enough to prevent dethreading of the string from macrocycle **17**, as was suggested by a CPK molecular model.

As in the case of pseudorotaxane **18**$^+$, a key step is the metal-directed threading process (i) of Figure 2, in which copper(I) forces the string to pass through the ring due to the strong tendency of this metal ion to form pseudotetrahedral bis-chelate complexes with two phen.

(a) Synthesis of the Ligands. The organic compounds used as precursors as well as the bifunctional molecular string are represented in Figure 3. 5,5″-Dimethyl-2,2′:6′,2″-terpyridine **1** was deprotonated with LDA in THF and then reacted with 2 equiv of THP-protected bromoethanol to afford **6** in 45% yield. An excess of base or alkylating agent, or prolonged reaction times, did not improve this yield. Deprotection with a catalytic amount of concentrated HCl in refluxing EtOH led to the corresponding diol **7** in high yield (white solid, 96%), which was transformed into the dimesylate **8** in 90% yield by reaction with MsCl and NEt_3 in CH_2Cl_2 at −2 °C. On the other hand, the phenolic blocking group **9** was prepared in three steps, from 4-bromo-*tert*-butylbenzene, methyl 4-*tert*-butylbenzoate, and phenol as reported in the literature.[20] Reaction of dimesylate **8** with **9** (1 equiv) in DMF at 75 °C in the presence of K_2CO_3 gave a mixture of mesylate **11** (46%), dialkylated product in which the two mesylates had been replaced by two blocking groups, and starting materials. During alumina column chromatography separation of this mixture, **11** was partially hydrolyzed to the corresponding alcohol **10**. Nevertheless, the latter could be easily converted again in mesylate **11** in almost quantitative yield by reaction with MsCl in the usual conditions (NEt_3, CH_2Cl_2, −2 °C). **11** was transformed into the more reactive bromo derivative **12** by reaction with anhydrous LiBr

(15) Jameson, D. L.; Guise, L. E. *Tetrahedron Lett.* **1991**, *32*, 1999−2002.
(16) Cárdenas, D. J.; Sauvage, J.-P. *Synlett* **1996**, 916−918.
(17) Dietrich-Buchecker, C. O.; Nierengarten, J.-F.; Sauvage, J.-P.; Armaroli, N.; Balzani, V.; De Cola, L. *J. Am. Chem. Soc.* **1993**, *115*, 11237−11244.
(18) Dietrich-Buchecker, C. O.; Sauvage, J.-P. *Tetrahedron* **1990**, *46*, 503−512.
(19) Dietrich-Buchecker, C. O.; Sauvage, J.-P.; Kern, J.-M. *J. Am. Chem. Soc.* **1989**, *111*, 7791−7800. Cárdenas, D. J.; Gavina, P.; Sauvage, J.-P. *J. Am. Chem. Soc.* **1997**, *119*, 2656−2664.
(20) Gibson, H. W.; Lee, S.-H.; Engen, P. T.; Lecavalier, P.; Sze, J.; Shen, Y. X.; Bheda, M. *J. Org. Chem.* **1993**, *58*, 3748−.

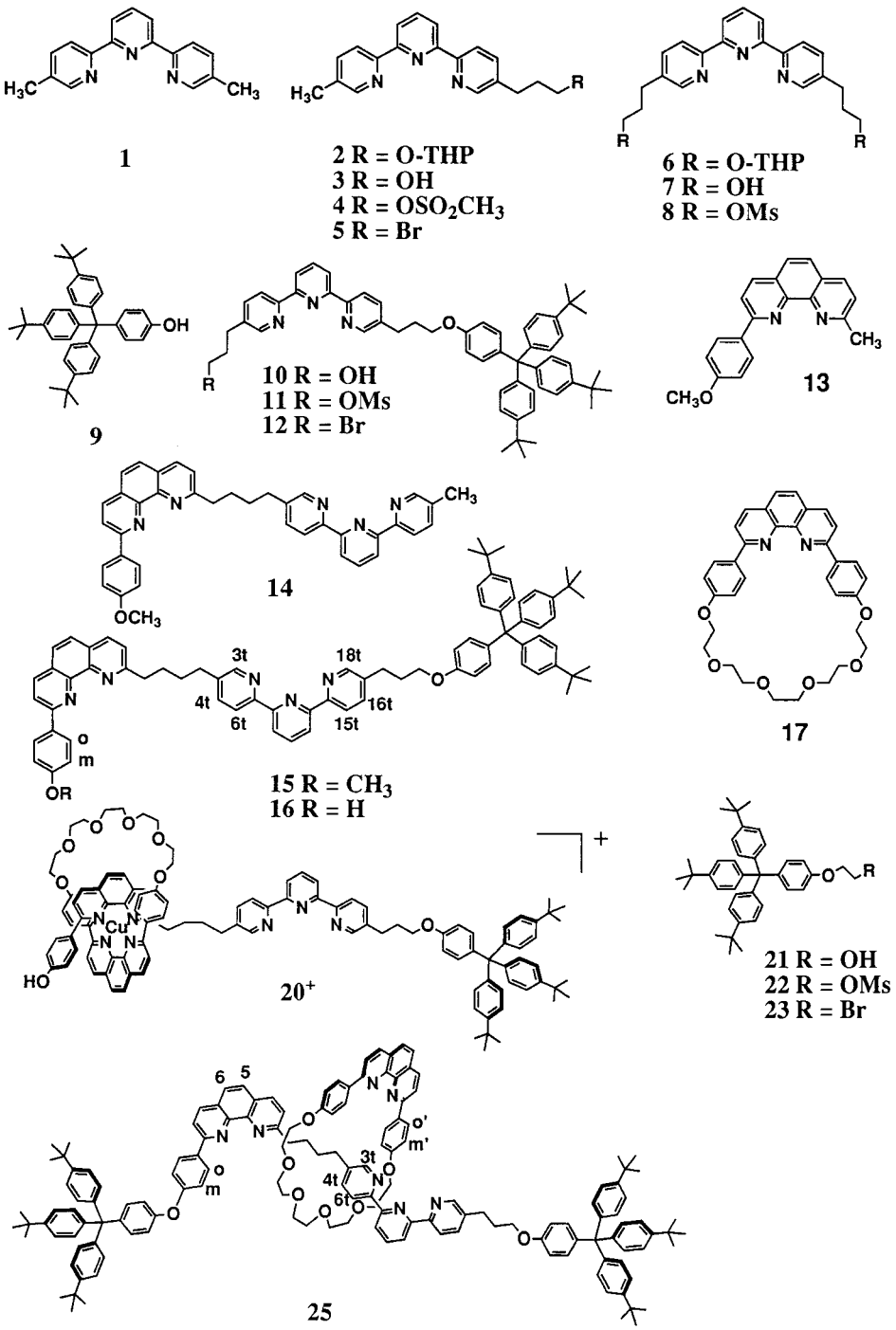

Figure 3. Intermediate compounds and demetalated rotaxane **25** synthesized.

in refluxing acetone. Finally, deprotonation of the phenanthroline-containing building block **13** with LDA in THF led to a deep red compound, which was further reacted with **12** in THF at room temperature to afford the desired string **15** (yellow solid, 61% isolated yield), incorporating a phen and a terpy unit and a stopper at one end.

(b) Synthesis of a Cu(I) Complex Semi-Rotaxane and Rotaxane. The coordinating macrocycle **17** was reacted with $Cu(MeCN)_4PF_6$ in CH_2Cl_2-MeCN under Ar at room temperature to give an orange solution of complex $Cu(\mathbf{17})(MeCN)_2PF_6$. Subsequent addition of a CH_2Cl_2 solution of string **15** led to semi-rotaxane $\mathbf{19}\cdot PF_6$ in almost quantitative yield, which was isolated as a red-brown solid. Again, as expected, the reaction proceeded regioselectively on the phen unit of the string, and no competition of the terpy ligand versus phen for Cu(I) was observed. This behavior was already observed in previous catenanes and related threaded systems[9,19] containing similar coordinating units.

For the preparation of the fully blocked rotaxane $\mathbf{24}^+$, ligand **15** was first demethylated by reaction with EtSNa in dry DMF at 110 °C to give the corresponding phenol **16** in 80% yield, as a yellow solid. **16** was then threaded into ring **17** by coordination to Cu(I) in the same way as for $\mathbf{19}^+$. The threaded four-coordinate copper(I) complex $\mathbf{20}^+$ was thus obtained in nearly quantitative yield as a brown-red solid. Separately, to effect the blocking reaction, we had first to convert **9** into an appropiate alkylating agent, able to react rapidly with the phenolic threaded system $\mathbf{20}^+$. Thus, **9** was allowed to react with THP-protected bromoethanol and K_2CO_3 in DMF, followed by deprotection with HCl to give alcohol **21** in 56% yield. This alcohol was

transformed into mesylate **22** (MsCl, NEt_3, CH_2Cl_2; 97%), which was further reacted with LiBr in refluxing acetone to obtain the corresponding bromo derivative **23** in nearly quantitative yield. Finally, the reaction of $\mathbf{20}^+$, **23**, and Cs_2CO_3 in DMF under Ar at 55 °C, followed by counterion exchange (KPF_6, H_2O, MeCN), led to rotaxane $\mathbf{24}\cdot PF_6$ in 40% yield.

Both threaded structures, $\mathbf{19}^+$ and $\mathbf{24}+$, were unambiguously characterized by FAB-MS and ^{1}H NMR and UV−vis spectroscopies. The ^{1}H NMR spectra of both systems are very similar. They both show the usual upfield shifts of the aromatic protons of the phenoxy moieties attached to the phenanthrolines, indicating the intertwined structures of the two phen around a copper(I). For instance, in rotaxane $\mathbf{24}^+$, the meta H signals appear at δ 5.97 ($4H_{m'}$) and 5.92 ($2H_m$), and the ortho H signals appear at δ 7.33 ($4H_{o'}$) and 7.11 ($2H_o$). Another interesting feature is that the protons of the phenanthroline central ring of the string ($H_{5,6}$) appear as two doublets with different chemical shifts (8.29 and 8.05 ppm), as shown by ^{1}H COSY experiments, while in string **15** both protons appear as one singlet (7.70 ppm, 2H). This different chemical environment of both protons in the threaded Cu(I) complexes could be due to some shift of the phen unit of the ring toward the phenoxy moiety attached to the phenantroline of the string to favor a better π-stacking. The protons of the first pyridine ring of the terpy moiety (H_{3t}, H_{4t}, and H_{6t}) closest to the phen also experience an upfield shift with respect to the free string, indicating that they could also be affected by the ring current of the phen nucleus of the ring. The UV−vis spectra of $\mathbf{19}^+$ and $\mathbf{24}^+$ show an absorption at 442 nm (ϵ = 3100 and 2700 M^{-1} cm^{-1}, respectively) characteristic of the $Cu(phen)_2^+$ species. FAB-MS confirmed the threaded structures. For semi-rotaxane $\mathbf{19}^+$, intense peaks are observed corresponding to the loss of the counterion (*m*/*z* 1747.8) and the loss of the counterion and the ring (*m*/*z* 1180.5). Similar features are observed for rotaxane $\mathbf{24}^+$. It is interesting to remark that no peaks are observed in the region lying between the peak corresponding to the loss of the counterion (*m*/*z* 2265.2) and the peak corresponding to the fragmentation and subsequent loss of the macrocycle from the thread (*m*/*z* 1698.0).

Demetalated Rotaxane 25. As has been previously reported, Cu(I) complex rotaxanes can be easily demetalated by reaction with cyanide in mild conditions, leading to rotaxanes with free coordination sites.[21] Thus, the reaction between $\mathbf{24}^+$ and KCN in a mixture of CH_2Cl_2−MeCN−H_2O at room temperature followed by column chromatography yielded the free rotaxane **25** as a white solid in 84% yield. The rotaxane structure was immediately confirmed by FAB-MS. As in the case of the Cu(I) complex rotaxane $\mathbf{24}^+$, no peaks are observed between the molecular ion (*m*/*z* 2202.1) and the peak corresponding to the fragmentation and loss of the ring (*m*/*z* 1635.9). This is a very characteristic feature of interlocked and threaded systems. In the ^{1}H NMR spectrum, we can observe a downfield shift of the aromatic protons of the phenoxy moieties attached to the phenanthrolines, indicating that the intertwined structure of the two phen around a copper(I) has disappeared. Thus, the meta protons appear at δ 6.90 ($4H_{m'}$) and 7.17 ($2H_m$) and the ortho at 8.31 and 8.29 ppm. These values are very close to the chemical shifts of the ring and the free string (ca. 8.40 ppm for H-ortho and 7.15 ppm for H-meta). Besides, the previously mentioned protons of the phenanthroline central ring of the string ($H_{5,6}$) appear now as a singlet, and the protons of the first pyridine ring of the terpy (H_{4t}, H_{6t}, and H_{3t}) are again downfield shifted to values close to those of the free string (δ 8.50−8.48 for H_{6t} and H_{18t}, 8.48−8.45 for H_{3t} and H_{15t}, and 7.61−7.57 for H_{4t} and H_{16t}).

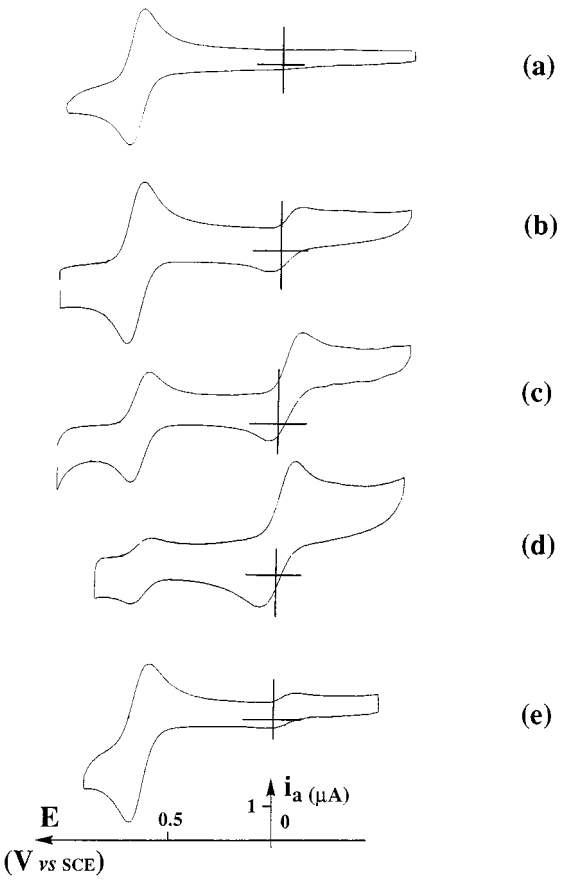

Figure 4. (a) Cyclic voltammogram of $\mathbf{24}^+$. (b) Same after electrolysis during 1 h at +1.0 V; (c and d) Evolution of $\mathbf{24}^{2+}$ solution with time: after 2 h (c) and after 4 h (d). (e) Cyclic voltammogram immediately after electrolysis of $\mathbf{24}^{2+}$ solution at −0.3 V. Conditions: MeCN (0.1 M, *n*-Bu_4NBF_4), Pt electrode, ν = 100 mV s^{-1}, 25 °C.

Electrochemically Driven Motion. From the previously determined electrochemical behavior of the catenane-type complexes,[9] and assuming some analogous values for the redox couples $Cu^{II}_{(4)}/Cu^{I}_{(4)}$ and $Cu^{II}_{(5)}/Cu^{I}_{(5)}$, we expect the same type of *electron-transfer-induced reaction*.[22]

In the three rotaxanes $\mathbf{18}^+$, $\mathbf{19}^+$, and $\mathbf{24}^+$, a square scheme, as depicted Figure 1, takes place. The electrochemical and chemical reactions are analyzed by cyclic voltammetry (CV) and controlled potential electrolysis experiments. From the CV measurements at differents scan rate (from 0.005 to 2 V s^{-1}) both on the copper(I) and on the copper(II) species, it could be inferred that the chemical steps (motions of the ring from the phenanthroline to the terpyridine and vice versa) are slow on the time scale of the experiments. As the two redox couples involved in these systems are separated by 0.7 V, the concentrations of the species in each environment (tetr-a or pentacoordination) are directly deduced from the peak intensities of the redox signals. In Figure 4 are displayed some voltammograms (curves a−e) obtained on different oxidation states of the rotaxane $\mathbf{24}^+$ and at different times.

Curve a diplays the voltammogram of a red solution of $\mathbf{24}^+$ in degassed acetonitrile. A reversible redox wave at 0.68 V (vs SCE) attests to the tetrahedral environment around the copper(I) atom.[9,14] During the potential scan, for rates between 0.005 and 2 V s^{-1}, no redox signal corresponding to the pentacoor-

(21) Dietrich-Buchecker, C. O.; Sauvage, J.-P. *Chem. Rev.* **1987**, *87*, 795−810. Chambron, J.-C.; Heitz, V.; Sauvage, J.-P. *J. Am. Chem. Soc.* **1993**, *115*, 12378−12384.

(22) Evans, D. H. *Chem. Rev.* **1990**, *90*, 739−751.

dination could be observed. This fact evidences the high kinetic stability of the four-coordinate copper(II) rotaxane generated at the electrode. At this stage, a controlled potential electrolysis (applied potential = +1.0 V) was performed until one Faraday was exchanged per mole of complex. During the electrolysis, the red color of the solution turned light green. Immediately after the coulometry, the voltammogram on the copper(II) species (curve b) showed the same redox couple at +0.68 V and an additional small reversible couple at −0.03 V. These signals are characteristic of the $Cu^{II}_{(4)}/Cu^{I}_{(4)}$ and $Cu^{II}_{(5)}/Cu^{I}_{(5)}$ couples, respectively.[9,14] After several hours at room temperature, without any visible color change, the progressive disappearance of the redox couple at +0.68 V (four-coordinate state) and the concomitant growth of the couple at −0.03 V (five-coordinate state) attest to the coordination change around the copper (II) ion (curves c and d). The analysis of the concentration of the two different copper(II) species with time leads to a first-order rate constant of 1.5×10^{-4} s^{-1} for the chemical reaction $Cu^{II}_{(4)}$, giving $Cu^{II}_{(5)}$. According to the invariant shape of the signals with the scan rate of the copper(II) solution, it can be inferred that the rate constant for the reaction $Cu^{I}_{(5)}$ to $Cu^{I}_{(4)}$ is smaller than 10^{-2} s^{-1}. A second electrolysis at −0.3 V restores the initial red solution. The voltammogram (curve e) performed immediately after the reductive electrolysis displays the redox couple of **24**$^+$ and is invariant with time. As all the $Cu^{I}_{(5)}$ species formed electrochemically are quantitatively transformed into $Cu^{I}_{(4)}$ species during the electrolysis, we can give a lower limit of 10^{-4} s^{-1} for the rate constante of the chemical reaction. The residual signal at −0.03 V simply reflects an incomplete electrolysis.

The behavior of the systems constituted by the unstoppered compound **18**$^+$, or the semirotaxane **19**$^+$,[13] is related to that of the fully blocked rotaxane **24**$^+$, i.e., the same redox couple can be observed. Some variations of peak intensities with the scan rate also indicate an acceleration of the chemical processes as compared to that of **24**$^+$. However, additional signals corresponding to the species $Cu^{I}(MeCN)_4^+$ ($E_{1/2}$ = +1.02 V) and $Cu^{II}_{(6)}$ (six-coordinate state, $E_{1/2}$ = −0.41 V)[14] reveal that the dethreading process becomes significant and occurs primarily with the copper(II) species. The six-coordinate complex evidenced by CV originates from the dethreading and coordination of the two linear fragments (**14** or **15**) via their terpy units to a copper center.

Of these three systems, **24**$^+$ is the most promising compound in relation with electrochemically induced molecular motions, due to the perfect chemical reversibility of the processes. Interestingly, the rates of the movements in rotaxane **24**$^+$ are very different from those measured for a related catenane.[14] The conversion $Cu^{II}_{(4)}$ to $Cu^{II}_{(5)}$ is faster in **24**$^+$ than that in the interlocking ring system previously described. This difference could reflect a greater ability of $Cu^{II}_{(4)}$ in **24**$^+$ to interact with solvent molecules or anions, the copper(II) center being perhaps loosely bound to a fifth ligand which would thus stabilize intermediate states on the way to $Cu^{II}_{(5)}$.

Photochemically Driven Motion. It is well known that Cu(I) complexes of polypyridine ligands absorb light throughout the UV−vis spectral region, display luminescence from the lowest triplet MLCT excited state, have a reasonably long lifetime, and can play the role of electron-transfer reductant.[23−25] This is also the case for the Cu(I)-based chromophoric unit of rotaxane **24**$^+$. It shows (i) UV absorption bands due to $\pi\pi^*$ ligand-centered (LC) transitions, (ii) metal-to-ligand charge-transfer (MLCT) bands in the 400−700-nm spectral region (Figure 5), and (iii) a MLCT emission band with λ_{max} = 785 nm and τ = 34 ns in aerated acetonitrile solution at 298 K (inset of Figure 5 and Table 1).

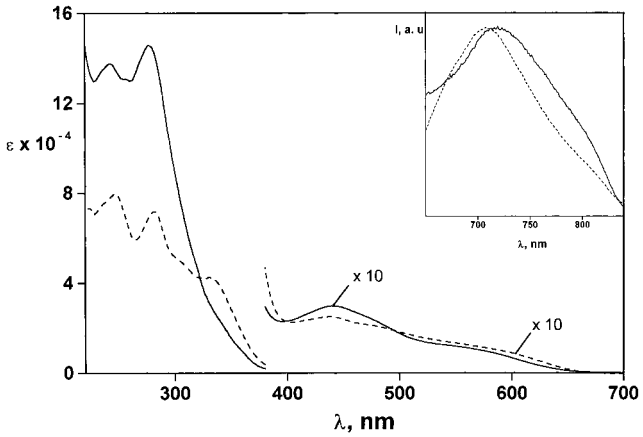

Figure 5. Absorption and (inset) uncorrected emission spectra in acetonitrile solution at 298 K of **24**$^+$ (full line) and of the analogous, previously studied copper(I) [2]-catenate **cat$_d$** (dashed line, see Chart 3 and ref 9). The stronger absorption of the rotaxane in the UV spectral region is due to the presence of the aromatic-type stoppers.

Table 1. Spectroscopic and Kinetic Parameters of the Rotaxane **24**$^+$ and the Analogous Catenate **cat$_d$** (see ref 9)[a]

	24$^+$	**cat$_d$**
λ_{max}(abs), nm[b]	439	439
ϵ_{max} (MLCT), M^{-1} cm^{-1}	3000	2300
λ_{max}(em), nm[c]	785	735
τ, ns	34	60
τ, ns[d]	64	115
k_q, M^{-1} cm^{-1} [e]	1.6×10^9	4.1×10^8
k_{conv} $Cu^{II}_{(4)}/Cu^{II}_{(5)}$, s^{-1} [f]	1.5×10^{-4}	2.8×10^{-5}
k_{conv} $Cu^{I}_{(5)}/Cu^{I}_{(4)}$, s^{-1} [g]	$10^{-4} \le k \le 10^{-2}$	1

[a] 298K, CH_3CN solution, unless otherwise noted. [b] Absorption maximun in the visible spectra region. [c] From emission maximun corrected for the photomultiplier response. [d] CH_2Cl_2 solution. [e] Bimolecular quenching constant obtained from Stern−Volmer plots, by using *p*-$NO_2C_6H_4CH_2Br$ as quencher; for more details, see text. [f] Rate constant for the conversion from the tetra- to pentacoordination of Cu(II), upon electrolysis of a solution of $Cu^{I}_{(4)}$. [g] Rate constant for the conversion from the penta- to tetracoordination of Cu(I), upon electrolysis of a solution of $Cu^{II}_{(5)}$.

The spectroscopic properties and excited-state properties of **24**$^+$ are similar, but not identical, to those of the analogous [2]-catenate, **cat$_d$** (Table 1 and Chart 3).[9]

The most remarkable difference is the shorter excited-state lifetime, which suggests that, in the rotaxane, the metal ion is

(23) (a) McMillin, D. R.; McNett, K. M. *Chem. Rev.* **1998**, *98*, 1201−1219. (b) Egglestone, M. K.; McMillin, D. R.; Koenig, K. S.; Pallenberg, A. J. *Inorg. Chem.* **1997**, *36*, 172−176. (c) Everly, R. M.; McMillin, D. R. *J. Phys. Chem.* **1991**, *95*, 9071−9075. (d) Gushurst, A. K. I.; McMillin, D. R.; Dietrich-Buchecker, C. O.; Sauvage, J.-P. *Inorg. Chem.* **1989**, *28*, 4070−4072. (e) Kirchhoff, J. R.; Gamache, R. E., Jr.; Blaskie, M. W.; Del Paggio, A. A.; Lengel, R. K.; McMillin, D. R. *Inorg. Chem.* **1983**, *22*, 2380−2384.

(24) (a) Kern, J.-M.; Sauvage, J.-P.; Weidmann, J.-L.; Armaroli, N.; Flamigni, L.; Ceroni, P.; Balzani, V. *Inorg. Chem.* **1997**, *36*, 5329−5338. (b) Dietrich-Buchecker, C. O.; Sauvage, J.-P.; Armaroli, N.; Ceroni, P.; Balzani, V. *Angew. Chem., Int. Ed. Engl.* **1996**, *35*, 1119−1121. (c) Armaroli, N.; Rodgers, M. A. J.; Ceroni, P.; Balzani, V.; Dietrich-Buchecker, C. O.; Kern, J.-M.; Bailal, Sauvage, J.-P. *Chem. Phys. Lett.* **1995**, *241*, 555−558. (d) Armaroli, N.; Balzani, V.; Barigelletti, F.; De Cola, L.; Flamigni, L.; Sauvage J.-P.; Hemmert, C. *J. Am. Chem. Soc.* **1994**, *116*, 5211−5217. (e) Dietrich-Buchecker, C. O.; Nierengarten, J.-F.; Sauvage, J.-P.; Armaroli, N.; Balzani, V.; De Cola, L. *J. Am. Chem. Soc.* **1993**, *115*, 11237−11244. (f) Armaroli, N.; De Cola, L.; Balzani, V.; Sauvage, J.-P.; Dietrich-Buchecker, C. O.; Kern, J.-M.; Bailal, A. *J. Chem. Soc., Dalton Trans.* **1993**, 3241−3247.

(25) Ruthkoski, M.; Castellano, F. N.; Meyer, G. J. *Inorg. Chem.* **1996**, *35*, 6406−6412.

Chart 3

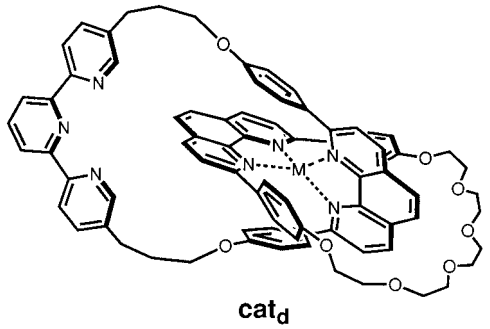

cat$_d$

less protected toward interaction with solvent molecules;[26,27] this is probably due to the lower number of phenyl substituents on the phenanthroline units of the rotaxane, with respect to the catenate.[9] Despite the shorter excited-state lifetime, we thought that it should be possible to cause the first step of the overall swinging process indicated in Figure 1, namely the conversion of **24**$^+$ into ***24**$^+$, by light irradiation in the presence of a suitable electron acceptor (A), as described by eqs 1−5:

$$\mathbf{24}^+ + h\nu \rightarrow {}^*\mathbf{24}^+ \quad (1)$$

$${}^*\mathbf{24}^+ \rightarrow \mathbf{24}^+ + \text{heat or } h\nu' \quad (2)$$

$${}^*\mathbf{24}^+ + \text{A} \rightarrow \mathbf{24}^{2+} + \text{A}^{\bullet -} \quad (3)$$

$$\mathbf{24}^{2+} + \text{A}^{\bullet -} \rightarrow \mathbf{24}^+ + \text{A} \quad (4)$$

$$\text{A}^{\bullet -} \rightarrow \text{products} \quad (5)$$

The occurrence of the excited-state electron-transfer process (eq 3) competes with nonradiative deactivation and luminescence (eq 2), which is therefore a useful handle to evaluate whether reaction 3 takes place. A necessary condition for the occurrence of reaction 3 is, of course, that it takes place with negative free energy change. The reduction potential of the **24**$^{2+}$/***24**$^+$ couple can be evaluated from the reduction potential of the **24**$^{2+}$/**24**$^+$ couple (+0.68 V in acetonitrile)[13] and the energy of the ***24**$^+$ excited state (about 1.58 eV, as estimated from the onset of the maximum of corrected emission band in the same solvent) by the following equation:[28]

$$E^\circ(\mathbf{24}^{2+}/{}^*\mathbf{24}^+) \sim E^\circ(\mathbf{24}^{2+}/\mathbf{24}^+) - \xi_{o-o} = -0.90 \text{ V} \quad (6)$$

where ξ_{o-o} is the energy of the ***24**$^+$ excited state as determined from the spectroscopic energy. This shows that even a mild oxidant should be capable of oxidizing the photoexcited ***24**$^+$ rotaxane (eq 3). As already pointed out, however,[9] the choice of the oxidant is not a trivial matter because other important requirements have to be satisfied: (i) the oxidant should not compete for light absorption, (ii) the reaction between ***24**$^+$ and the oxidant (eq 3) should be fast enough to compete with the intrinsic excited-state decay (eq 2), and (iii) after reduction, the oxidant should undergo a very fast, irreversible decomposition reaction (eq 5) in order to prevent the occurrence of the back-electron-transfer reaction (eq 4). Such requirements are substantially met by *p*-$NO_2C_6H_4CH_2Br$ (*p*-nitrobenzylbromide),[29,30] which was successfully used to cause photooxidation of the analogous catenane.[9] A Stern−Volmer analysis[31] of the quenching of the luminescence of ***24**$^+$ by *p*-$NO_2C_6H_4CH_2Br$ showed that the rate constant of the quenching process (eq 3) is 1.6×10^9 M^{-1} s^{-1} in acetonitrile solution at 298 K, i.e., much larger than that found in the case of the catenane species[9] (Table 1). This compensates for the shorter excited-state lifetime of the rotaxane and allows its photooxidation to occur in a relatively short time when a sufficiently high concentration of *p*-$NO_2C_6H_4CH_2Br$ is present in the solution. The principle of the photochemically triggered rearrangement of the rotaxane **24**$^+$ is given Figure 6.

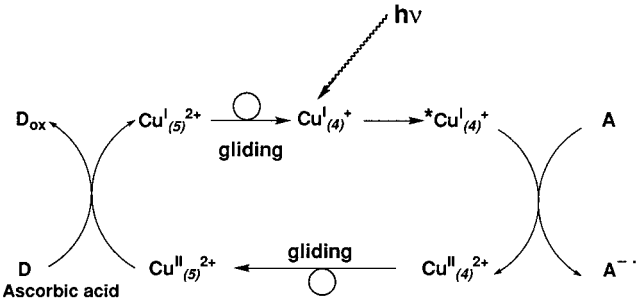

Figure 6. Principle of the photochemically and chemically triggerred rearrangement of the rotaxane **24**$^+$.

Photochemical experiments were performed by irradiating with 464-nm light acetonitrile solutions containing 1.0×10^{-4} M **24**$^+$ and 1.8×10^{-2} M *p*-$NO_2C_6H_4CH_2Br$. Under these conditions, all the exciting light is absorbed by the Cu(I) catenate. Light irradiation was found to cause spectral changes indicating the disappearance of the Cu(I) species within 20 min, but no isosbestic point was present, contrary to what was found for the analogous catenate.[9] At the end of the photoreaction, the irradiated solution was kept in the dark at 298 K; meanwhile, the occurrence of a very slow reaction was evidenced by spectrophotometric measurements. The final spectrum (after 24 h) was reminiscent of, but clearly different from, that found upon photochemical oxidation of the analogous catenate and, more generally, that exhibited by the $[Cu(phen)_2]^{2+}$-type chromophoric units.[23,24,32] At this stage, addition of an excess of ascorbic acid (dissolved in MeOH) caused a gradual, slow increase of the absorption spectrum in the 400−600-nm region, but only about 70% of the initial **24**$^+$ species was recovered when no further spectral changes were observed (after about 4 h). These results indicate that, under the experimental conditions used, a substantial part of the Cu ions lose pyridine-type coordination. The reason for such a behavior was not immediately clear since the electrochemically driven oxidation−reduction cycle is fully reversible. From the experimental viewpoint, the only difference was that the electrochemical processes were carried out in the presence of tetrabutylammonium tetrafluoroborate (TBA(BF_4)) as supporting electrolyte,

(26) (a) Everly, R. M.; McMillin, D. R. *Photochem. Photobiol.* **1989**, *50*, 711−. (b) Kirchhoff, J. R.; McMillin, D. R.; Robinson, W. R.; Powell, D. R.; McKenzie, A. T.; Chen, S. *Inorg. Chem.* **1985**, *24*, 3928−3933.

(27) Miller, M. T.; Gantzel, P. K.; Karpishin, T. B. *Inorg. Chem.* **1998**, *37*, 2285−2290.

(28) Balzani, V.; Bolletta, F.; Gandolfi, M. T.; Maestri, M. *Top. Curr. Chem.* **1978**, *75*, 1−64.

(29) In acetonitrile solution, *p*-$NO_2C_6H_4CH_2Br$ shows a band with $\lambda_{max} = 273$ nm which does not interfere in the visible light absorption of Cu^IN_4. On reduction of *p*-$NO_2C_6H_4CH_2Br$, a benzylic radical is formed which undergoes a fast dimerization reaction. In the presence of dioxygen, the benzylic radical gives rise to a series of reactions which end with formation of benzaldehyde.[30]

(30) Kern, J.-M.; Sauvage, J.-P. *J. Chem. Soc., Chem. Commun.* **1987**, 546−548.

(31) (a) Stern, O.; Volmer, M. *Z. Phys.* **1919**, *20*, 183. (b) Gilbert, A.; Baggott, J. *Essentials of Molecular Photochemistry*; Blackwell Scientific Publications: Oxford, U.K., 1991.

(32) (a) Phifer, C. C.; McMillin, D. R. *Inorg. Chem.* **1986**, *25*, 1329−1333. (b) Karlsson, K.; Moucheron, C.; Kirsch-De Mesmaeker, A. *New J. Chem* **1994**, *18*, 721−729.

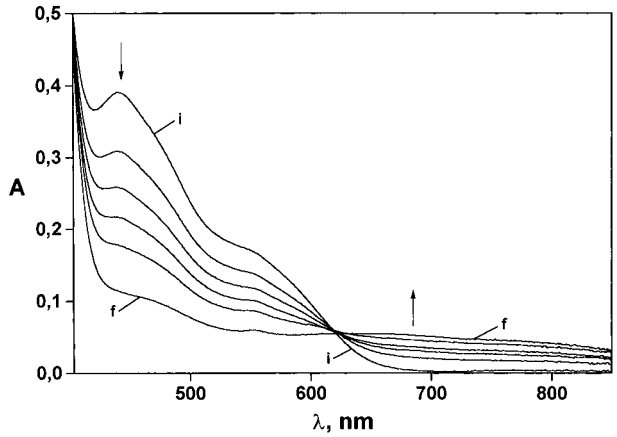

Figure 7. Spectral changes caused by photoirradiation of an acetonitrile solution containing 1.0×10^{-4} M **24**$^{+}$, 1.8×10^{-2} M *p*-$NO_2C_6H_4CH_2$-Br, and 1.0×10^{-1} M TBA(BF_4). The isosbestic point is at 626 nm. (i) Initial spectrum; (f) final spectrum obtained after 20 min of irradiation.

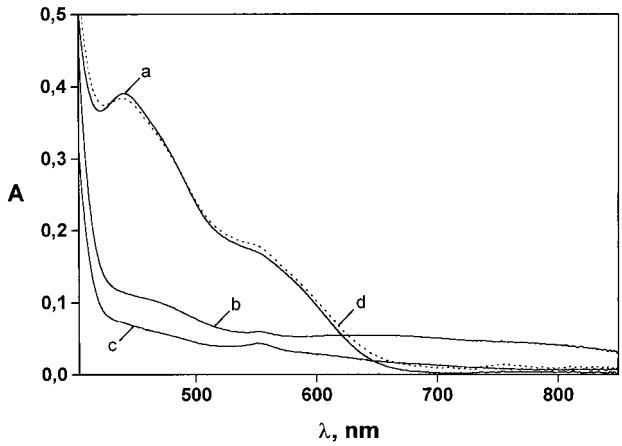

Figure 8. Absorption spectra of an acetonitrile solution of **24**$^{+}$ containing 1.0×10^{-1} M TBA(BF_4): (a) before light irradiation; (b) at the end of the photoreaction (about 20 min irradiation) with *p*-$NO_2C_6H_4CH_2Br$; (c) after subsequent 26 h in the dark; (d) 8 h after subsequent addition of an excess of ascorbic acid.

whereas such a salt was not present under the photochemical conditions. We have previously found that, in the analogous catenate system,[9] the rate of the structural rearrangement processes is strongly affected by the nature of the solvent and the presence of salts, presumably because the change in the coordination number of the metal requires solvent/anion assistance. Such assistance is likely to be more important in the rotaxane than in the catenate because, in the former, the gliding motions imply a shift of the copper ion along the thread with a complete lack of a chelating unit. Therefore, we thought that the different behavior found for the photoinduced compared to the electrochemically induced process in the rotaxane could be due to the absence and, respectively, presence of TBA(BF_4).

To check this hypothesis, we carried out a new series of photochemical experiments in the presence of 0.1 M TBA(BF_4). Under these conditions, light excitation was found to cause the spectral changes shown in Figure 7, which clearly indicate the disappearance of **24**$^{+}$ and the concomitant formation of **24**$^{2+}$-($Cu^{II}_{(4)}$) as the only reaction product. At the end of the photoreaction, the irradiated solution was kept in the dark at 298 K. Spectrophotometric measurements showed that a slow reaction was occurring, causing a general decrease in absorbance, particularly in the 600−800-nm region (Figure 8), as expected for the transformation of **24**$^{2+}$($Cu^{II}_{(4)}$) into the more stable **24**$^{2+}$($Cu^{II}_{(5)}$) species (Figure 6). After about 26 h, no further spectral change was observed. At this stage, the spectrum of the solution was that shown by curve c in Figure 8, which is that of the stable $Cu^{II}_{(5)}$ species. To close the cycle (Figure 6), an excess of ascorbic acid was added to the solution. A gradual, complete reappearance of the spectrum of **24**$^{+}$($Cu^{I}_{(4)}$) was observed, as happens when oxidation and successive reduction are carried out electrochemically. After about 8 h, the spectrum was practically coincident with the initial spectrum (Figure 8), showing that the cyclic process (Figure 6) is fully reversible, even when oxidation is photoinduced and reduction is chemically induced.[33]

The overall quantum yield of the photoreaction was about 3%. Since, under the experimental conditions used, the fraction of ***24**$^{+}$ excited states reacting with the quencher is ∼50%, the fraction of quenching events that give rise to a permanent formation of **24**$^{2+}$ is ∼6%. Since *p*-$NO_2C_6H_4CH_2Br$ cannot quench ***24**$^{+}$ by energy transfer, the low efficiency of the photoinduced process has to be attributed to a competition between back electron transfer (reaction 4) and the irreversible decomposition of the primary reduced product of *p*-$NO_2C_6H_4$-CH_2Br (reaction 5).

Conclusion

The motion of the ring and of the metal ion from the bidentate to the tridentate site on the string can be carried out electrochemically or by an oxidative photochemical process and can be fully reversed upon chemical reduction. A comparison with the analogous catenate **cat$_d$**[9] shows that, for **24**$^{+}$, (i) the excited-state lifetime is shorter, (ii) the rate constant for the excited-state quenching reaction by *p*-$NO_2C_6H_4CH_2Br$ is higher, and (iii) the thermal $Cu^{II}_{(4)}$/$Cu^{II}_{(5)}$ conversion is less clean in the absence of TBA(BF_4). These results show that the metal ion is less protected from interaction with external species in the rotaxane than in the catenate, as expected from structural considerations. This is also in agreement with the faster and, respectively, slower rate constant observed for the $Cu^{II}_{(4)}$-to-$Cu^{II}_{(5)}$ and the $Cu^{I}_{(5)}$-to-$Cu^{I}_{(4)}$ conversions in the rotaxane compared to the catenane species.

Experimental Section

Materials and General Procedures. The following chemicals were prepared according to literature procedures: 5,5″-dimethyl-2,2′:6′,2″-terpyridine (**1**),[9] 2-methyl-9-(*p*-anisyl)-1,10-phenanthroline (**13**),[17] Cu(MeCN)$_4BF_4$,[18] Cu(MeCN)$_4PF_6$,[34] and tris(*p-tert*-butylphenyl)(4-hydroxyphenyl)methane (**9**).[20] All other chemicals were of the best commercially available grade and were used without further purification. Dry solvents were distilled from suitable desiccants (DMF from CaH_2 under reduced pressure, CH_2Cl_2 from P_2O_5 or CaH_2, THF from Na and benzophenone). Thin-layer chromatography (TLC) was carried out on aluminum sheets coated with silica gel 60 F_{254} (Merck 5554) or on plastic sheets precoated with aluminum oxide N/UV_{254} (Macherey Nagel 802021). After elution, the plates were either examined under a UV lamp or exposed to I_2. Column chromatography was performed with silica gel 60 (Merck 9385, 230−400 mesh) or aluminum oxide 90 (neutral, act. II−III, Merck 1097). ^{1}H NMR spectra were recorded on either Bruker WP 200SY (200 MHz) or WP 400SY (400 MHz) spectrometers (using the deuterated solvent as the lock and residual solvent as the internal reference). Fast atom bombardment mass spectra (FAB-MS) were recorded in the positive ion mode with either a krypton primary atom beam in conjunction with a 3-nitrobenzyl alcohol matrix and a Kratos MS80RF mass spectrometer coupled to a DS90 system,

(33) Since **24**$^{2+}$ is not photosensitive and does not exhibit any long-lived excited state, the reduction step cannot be induced by light; see ref 9.

(34) Kubas, G. J.; Monzik, B.; Crumbliss, A. *Inorg. Synth.* **1990**, *28*, 68−70.

or a xenon primary atom beam with the same matrix and a ZAB-HF mass spectrometer. Melting points were mesured with a Büchi SMP20 apparatus and are uncorrected. Electrochemical measurements were performed with a three-electrode system consisting of a platinum working electrode, a platinum wire counter electrode, and a standard reference calomel electrode (SCE), versus which all potentials are reported. All measurements were carried out under Ar, in degassed spectroscopic grade solvents, using 0.1 M *n*-Bu_4NBF_4 solutions as supporting electrolyte. An EG&G Princeton Applied Research model 273A potentiostat connected to a computer was used (software from Program Research Electrochemistry Software), as well as a Bruker E130M potentiostat, connected to a printing table.

All the spectroscopic and photochemical investigations were carried out in 1-cm-path length cuvettes using acetonitrile as solvent (Carlo Erba for spectroscopy). The absorption spectra were recorded with a Perkin-Elmer Lambda-5 spectrophotometer. Emission spectra were obtained with a Spex Fluorolog II spectrofluorometer (continuous Xe lamp, Osram XBOW/1), equipped with a Hamamatsu R-928 photomultiplier tube. For the photochemical experiments, the concentration of $\mathbf{24}^+$ (as PF_6^- salt) was 1.0×10^{-4} M, and that of *p*-$NO_2C_6H_4CH_2Br$ was 1.8×10^{-2} M. The solutions, continuously stirred, were irradiated with the spectrofluorometer lamp (see above) at 464 nm (1681B minimate Spex monochromator) using slits of 2.5 mm (9.4 nm).The quantum yield of the photoreaction was calculated by measuring the intensity of the light source with the "microversion" of the ferric oxalate actinometer.[35] An IBH single-photon-counting equipment N_2 lamp (λ_{exc} = 337 nm) was used to obtain the excited-state lifetimes.

5″-Methyl-5-{3-[(tetrahydro-2*H*-pyran-2-yl)oxy]-1-propyl}-2,2′:6′2″-terpyridine (2). A titrated commercial solution of LDA in THF (ca. 1.5 M, 20.2 mL, 30.3 mmol) was slowly added dropwise to a solution of 5,5″-dimethyl-2,2′:6′,2″-terpyridine **1** (7.15 g, 27.4 mmol) in anhydrous THF (275 mL) at −78 °C. The resulting deep purple solution was stirred under Ar for 2 h at −78 °C and then for 0.5 h at 0 °C. After the solution was cooled back to −78 °C, a degassed solution of 2-(2-bromoethoxy)tetrahydro-2*H*-pyran (5.72 g, 27.4 g mmol) in anhydrous THF (270 mL) at 0 °C was added by means of a double-ended needle. The resulting mixture was left at 0 °C and allowed to reach room temperature with stirring for 16 h. Then it was cooled back to 0 °C, and 100 mL of H_2O was slowly added. THF was evaporated, and the residue was taken in CH_2Cl_2, washed with water, dried over $MgSO_4$, and filtered. Solvent was evaporated, and the residue was subjected to column chromatography on alumina (hexanes−Et_2O), yielding **2** (4.66 g, 44%) as a white solid: mp 67−69 °C; ^{1}H NMR (200 MHz, $CDCl_3$) δ = 8.55−8.49 (m, 4H), 8.39 (d, *J* = 7.8 Hz, 2H), 7.93 (t, *J* = 7.9 Hz, 1H), 7.72−7.64 (m, 2H), 4.60 (t, *J* = 3.0 Hz, 1H), 3.95−3.77 (m, 2H), 3.58−3.39 (m, 2H), 2.82 (t, *J* = 7.3 Hz, 2H), 2.42 (s, 3H), 1.99 (qt, *J* = 7.4 Hz, 2H), 1.91−1.50 (m, 6H); ^{13}C{^{1}H} NMR (50 MHz, $CDCl_3$, DEPT) δ = 155.5 (2C), 154.3 (C), 153.9 (C), 149.6 (CH), 149.4 (CH), 137.8 (CH), 137.5 (C), 137.4 (CH), 136.8 (CH), 133.4 (C), 120.9 (CH), 120.7 (CH), 120.4 (2CH), 99.1 (CH), 66.5 (CH_2), 62.5 (CH_2), 31.1 (CH_2), 30.8 (CH_2), 29.6 (CH_2), 25.5 (CH_2), 19.8 (CH_2), 18.4 (CH_3); EI-MS *m*/*z* (relative intensity) 389 (10, M^+), 360 (11), 334 (8), 287 (69), 274 (73), 261 (100).

5-(3-Hydroxy-1-propyl)-5″-methyl-2,2′:6′,2″-terpyridine (3). A solution of **2** (5.11 g, 13.1 mmol) in EtOH (300 mL) was heated to reflux. Concentrated HCl (0.5 mL) was added, and the mixture was refluxed for 3 h. The solution was allowed to cool to room temperature and then neutralized with concentrated NaOH (ca. 30%). EtOH was evaporated, and the residue was taken in CH_2Cl_2 and washed with brine. The organic phase was dried over Na_2SO_4 and filtered. Evaporation of the solvent led to a yellow solid (3.78 g) which was purified by column chromatography on alumina (CH_2Cl_2 containing 0−1% MeOH) to give pure alcohol **3** (3.40 g, 85%) as a white powder: mp 111−112 °C; ^{1}H NMR (200 MHz, $CDCl_3$) δ = 8.53−8.47 (m, 4H), 8.37 (d, *J* = 7.8 Hz, 2H), 7.92 (t, *J* = 7.8 Hz, 1H), 7.70−7.62 (m, 2H), 3.70 (t, *J* = 6.3 Hz, 2H), 2.79 (t, *J* = 7.7 Hz, 2H), 2.40 (s, 3H), 2.10 (br s, 1H), 1.99−1.85 (m, 2H); ^{13}C{^{1}H} NMR (50 MHz, $CDCl_3$, DEPT δ = 155.4 (C), 155.3 (C), 154.2 (C), 153.7 (C), 149.5 (CH), 149.2 (CH), 137.8 (CH), 137.6 (C), 137.5 (CH), 136.9 (CH), 133.5 (C), 121.0 (CH), 120.9 (CH), 120.5 (2 CH), 61.5 (CH_2), 33.8 (CH_2), 29.1 (CH_2), 18.4 (CH_3); EI-MS *m*/*z* (relative intensity) 305 (100, M^+), 287 (18), 286 (38), 275 (35), 274 (45), 260 (65), 143 (20). Anal. Calcd for $C_{19}H_{19}N_3O$: C, 74.73; H, 6.27; N, 13.76. Found: C, 74.63; H, 6.19; N, 13.61.

5-(3-Methanosulfonyl-1-propyl)-5″-methyl-2,2′:6′,2"-terpyridine (4). A solution of **3** (3.38 g, 11.1 mmol) and freshly distilled NEt_3 (9.3 mL, 66.6 mmol) in anhydrous CH_2Cl_2 (300 mL) was cooled to −3 °C. Mesyl chloride (3.5 mL, 44.4 mmol) in anhydrous CH_2Cl_2 (85 mL) was added dropwise (−5 °C < *T* < −2 °C), and the resulting mixture was stirred under Ar at −3 °C for 4 h. The reaction mixture was washed with cold H_2O and dried over Na_2SO_4. The organic phase was filtered and concentrated to furnish a white solid, which was purified through a short alumina column (CH_2Cl_2) to give **4** as a white powder (4.05 g, 95%): mp 92−94 °C; ^{1}H NMR (200 MHz, $CDCl_3$) δ = 8.58−8.48 (m, 4H), 8.40 (d, *J* = 7.8 Hz, 2H), 7.93 (t, *J* = 7.8 Hz, 1H), 7.72−7.64 (m, 2H), 4.29 (t, *J* = 6.2 Hz, 2H), 3.03 (s, 3H), 2.86 (t, *J* = 7.6 Hz, 2H), 2.42 (s, 3H), 2.22−2.08 (m, 2H); ^{13}C{^{1}H} NMR (50 MHz, $CDCl_3$, DEPT) δ = 155.4 (C), 155.2 (C), 154.7 (C), 153.7 (C), 149.5 (CH), 149.2 (CH), 137.9 (CH), 137.6 (CH), 137.0 (CH), 135.9 (C), 133.6 (C), 121.1 (CH), 120.8 (CH), 120.7 (CH), 120.6 (CH), 68.7 (CH_2), 37.5 (CH_3), 30.5 (CH_2), 28.7 (CH_2), 18.5 (CH_3); EI-MS *m*/*z* (relative intensity) 383 (45, M^+), 287 (49), 286 (52), 274 (100), 260 (38).

5-(3-Bromo-1-propyl)-5″-methyl-2,2′:6′2″-terpyridine (5). A mixture of **4** (0.45 g, 1.17 mmol) and anhydrous LiBr (0.51 g, 5.9 mmol) in acetone (30 mL) was refluxed under Ar for 1 h. After evaporation of the solvent, the crude mixture was dissolved in CH_2Cl_2, washed with H_2O, and dried over Na_2SO_4. Solvent was evaporated to yield a white solid (0.416 g, 97%), which was used in the next step without further purification: ^{1}H NMR (200 MHz, $CDCl_3$) δ = 8.57−8.48 (m, 4H), 8.39 (d, *J* = 7.6 Hz, 2H), 7.93 (t, *J* = 7.8 Hz, 1H), 7.73−7.64 (m, 2H), 3.44 (t, *J* = 6.4 Hz, 2H), 2.89 (t, *J* = 7.4 Hz, 2H), 2.42 (s, 3H), 2.30−2.16 (m, 2H).

Ligand 14. A titrated commercial solution of LDA in THF (ca. 1.3 M, 1.05 mL, 1.35 mmol) was added dropwise to a stirred solution of 2-methyl-9-(*p*-anisyl)-1,10-phenanthroline **13** (0.40 g, 1.33 mmol) in anhydrous THF (20 mL) at −78 °C. The resulting deep red solution was stirred under Ar for 2 h at −78 °C and then for 1 h from −78 to 10 °C. After the solution was cooled back to −78 °C, a degassed solution of **5** (0.41 g, 1.11 mmol) in anhydrous THF (20 mL) was added dropwise. The reaction mixture was left in an ice bath and allowed to reach room temperature with stirring overnight. The resulting blue solution was hydrolyzed at 0 °C with 10 mL of H_2O. THF was evaporated and the residue extracted with CH_2Cl_2. The combined organic layers were washed with water, dried over Na_2SO_4, and filtered. Solvent was evaporated to give an orange oil which was purified by column chromatography on alumina (hexane−CH_2Cl_2) to yield **14** (0.364 g, 56%), as a yellow solid: ^{1}H NMR (400 MHz, $CDCl_3$) δ = 8.57 (d, *J* = 2 Hz, 1H), 8.52 (d, *J* = 2 Hz, 1H), 8.50 (d, *J* = 8.0 Hz, 1H), 8.48 (d, *J* = 8.0 Hz, 1H), 8.39−8.35 (m, 4H), 8.24 (d, *J* = 8.5 Hz, 1H), 8.14 (d, *J* = 8.2 Hz, 1H), 8.05 (d, *J* = 8.5 Hz, 1H), 7.91 (t, *J* = 7.8 Hz, 1H), 7.75−7.70 (m, 3H), 7.64 (dd, *J* = 8.0 and 2 Hz, 1H), 7.50 (d, *J* = 8.2 Hz, 1H), 7.07 (d, *J* = 8.8 Hz, 2H), 3.87 (s, 3H), 3.28 (t, *J* = 7.8 Hz, 2H), 2.85 (t, *J* = 7.6 Hz, 2H), 2.41 (s, 3H), 2.10 (qt, *J* = 7.8 Hz, 2H), 1.92 (qt, *J* = 7.6 Hz, 2H); FAB-MS *m*/*z* (relative intensity) 588.2 (100, MH^+), 313.1 (10, M − $C_{18}H_{16}N_3$), 300.1 (16, M − $C_{19}H_{17}N_3$), 287.1 (15, $C_{19}H_{17}N_3$), 274.1 (12, $C_{18}H_{16}N_3$).

Pseudorotaxane 18·BF_4. A solution of $Cu(MeCN)_4BF_4$ (0.065 g, 0.207 mmol) in degassed MeCN (35 mL) was transferred by means of a double-ended needle to a degassed solution of macrocycle **17** (0.122 g, 0.216 mmol) in CH_2Cl_2 (35 mL) under Ar. The mixture turned orange instantaneously. After the mixture was stirred at room temperature for 20 min, a degassed solution of **14** (0.127 g, 0.216 mmol) in CH_2Cl_2 (35 mL) under Ar was added via a double-ended needle, resulting in the immediate formation of a dark red solution. The reaction mixture was stirred overnight under Ar at room temperature. After evaporation of the solvents, the residue was chromatographed on an alumina column (CH_2Cl_2−0.5% MeOH), yielding **18**·BF_4 (0.212 g, 75%) as a brown-red solid: ^{1}H NMR (200 MHz, CD_2Cl_2) δ = 8.67 (d, *J* = 8.3 Hz, 1H), 8.55−7.65 (m, 19H), 7.57 (d, *J* = 8.3 Hz, 1H), 7.31 (d, *J* = 8.6 Hz, 4H), 7.14 (d, *J* = 8.7 Hz, 2H), 5.95 (d, *J* = 8.6 Hz, 4H), 5.88 (d, *J* =

(35) Fisher, E. *EPA Newsl.* **1983**, July, 33−34.

8.7 Hz, 2H), 3.80 (s, 4H), 3.70−3.38 (m, 16H), 3.46 (s, 3H), 2.50 (t, J = 7.8 Hz, 2H), 2.43 (s, 3H), 2.29 (t, J = 7.8 Hz, 2H), 1.55−1.45 (m, 2H), 1.30−1.20 (m, 2H); UV−vis (MeCN) λ_{max} = 442 nm (ϵ 3100); FAB-MS *m*/*z* (relative intensity) 1216.4 (39, $[M - BF_4]^+$; calcd 1216.4), 650.2 (100, $[M - \mathbf{17} - BF_4]^+$; calcd 650.2), 629.1 (28, $[M - \mathbf{14} - BF_4]^+$; calcd 629.2), 588.2 (12, $\mathbf{14}H^+$; calcd 588.3), 567.2 (17, $\mathbf{17}H^+$; calcd 567.2).

5,5″-Bis{3-[(tetrahydro-2*H*-pyran-2-yl)oxy]-1-propyl}-2,2′:6′,2″-terpyridine (6). A titrated commercial solution of LDA in THF (ca. 1.5 M, 5.6 mL, 8.4 mmol) was slowly added dropwise over a solution of 5,5″-dimethyl-2,2′:6′,2″-terpyridine **1** (1.0 g, 3.83 mmol) in anhydrous THF (40 mL) at −78 °C. The resulting purple solution was stirred under Ar for 2 h at −78 °C and for 0.5 h at 0 °C. Then it was cooled again to −78 °C, and a degassed solution of THP-protected bromoethanol (1.76 g, 8.42 mmol) in anhydrous THF (40 mL) at 0 °C was added under Ar by means of a double-ended needle. The resulting mixture was left at 0 °C and allowed to reach room temperature with stirring for 16 h. The blue solution thus obtained was hydrolyzed at 0 °C with 30 mL of H_2O. THF was evaporated and the residue extracted with CH_2Cl_2, dried over Na_2SO_4, and filtered. Evaporation of the solvent led to an orange solid which was subjected to column chromatography on alumina (ether−hexane) to afford **6** (0.89 g, 45%) as a white solid: mp 71−73 °C; ^{1}H NMR (200 MHz, $CDCl_3$) δ = 8.55 (br s, 2H), 8.53 (d, J = 7.8 Hz, 2H), 8.39 (d, J = 7.8 Hz, 2H), 7.93 (t, J = 7.8 Hz, 1H), 7.69 (dd, J = 7.8 and 2.3 Hz, 2H), 4.60 (t, J = 3.5 Hz, 2H), 3.93−3.77 (m, 4H), 3.56−3.39 (m, 4H), 2.81 (t, J = 7.2 Hz, 4H), 1.99 (qt, J = 7.2 Hz, 4H), 1.92−1.50 (m, 12H); ^{13}C NMR (50.3 MHz, $CDCl_3$, DEPT) δ = 155.5 (C), 154.3 (C), 149.4 (CH), 137.8 (CH), 137.5 (C), 136.8 (CH), 120.9 (CH), 120.5 (CH), 99.1 (CH), 66.5 (CH_2), 62.5 (CH_2), 31.1 (CH_2), 30.8 (CH_2), 29.6 (CH_2), 25.5 (CH_2), 19.8 (CH_2).

5,5″-Bis(3-hydroxy-1-propyl)-2,2′:6′,2″-terpyridine (7). Concentrated HCl (0.3 mL) was added to a refluxing solution of **6** (1.89 g, 3.65 mmol) in EtOH (100 mL). The mixture was refluxed for 3 h and then allowed to reach room temperature with stirring overnight. After neutralization with concentrated NaOH, EtOH was removed and the residue taken in CH_2Cl_2 and washed with brine. Solvent was partially evaporated, resulting in the precipitation of a white solid, which was separated by filtration (0.98 g). The filtered organic phases were gathered. Solvent was evaporated and the residue purified by column chromatography (alumina, CH_2Cl_2−2% MeOH) to give other 0.25 g of white solid (overall yield of **7,** 96%). A small amount was recrystallized from CH_2Cl_2, affording white needles of **7**: mp 131−132 °C; ^{1}H NMR (200 MHz, $CDCl_3$) δ = 8.56 (br s, 2H), 8.53 (d, J = 7.8 Hz, 2H), 8.39 (d, J = 7.8 Hz, 2H), 7.94 (t, J = 7.8 Hz, 1H), 7.70 (dd, J = 7.8 and 2.3 Hz, 2H), 3.73 (q, $J \approx$ 5.9 Hz, 4H), 2.81 (t, J = 7.7 Hz, 4H), 2.02−1.88 (m, 4H), 1.40 (t, J = 5.1 Hz, 2H); ^{13}C NMR (50.3 MHz, $CDCl_3$) δ = 155.4 (C), 154.4 (C), 149.3 (CH), 137.9 (CH), 137.5 (C), 136.8 (CH), 120.9 (CH), 120.6 (CH), 61.9 (CH_2), 33.9 (CH_2), 29.1 (CH_2). Anal. calcd for $C_{21}H_{23}N_3O_2$: C, 72.18; H, 6.63; N, 12.03. Found: C, 72.22; H, 6.69; N, 11.88.

5,5″-Bis(3-methanosulfonyl-1-propyl)-2,2′:6′,2″-terpyridine (8). Mesyl chloride (0.93 mL, 12 mmol) in anhydrous CH_2Cl_2 (20 mL) was slowly added dropwise over a stirred solution of diol **7** (0.524 g, 1.50 mmol) and freshly distilled NEt_3 (2.51 mL, 18 mmol) in anhydrous CH_2Cl_2 (40 mL) at −3 °C. The resulting mixture was stirred under Ar at −2 °C for 4 h. The reaction mixture was then washed with cold H_2O, dried over Na_2SO_4, and filtered. Removal of the solvent led to a yellow solid, which was filtered through a short alumina column (CH_2Cl_2) to give a white solid (0.68 g, 90%): ^{1}H NMR (200 MHz, $CDCl_3$) δ = 8.58−8.54 (m, 4H), 8.41 (d, J = 7.8 Hz, 2H), 7.95 (t, J = 7.8 Hz, 1H) 7.71 (dd, J = 7.8 and 2.2 Hz, 2H), 4.30 (t, J = 6.2 Hz, 4H), 3.04 (s, 6H), 2.87 (t, J = 7.5 Hz, 4H), 2.21−2.11 (m, 4H); ^{13}C NMR (50.3 MHz, $CDCl_3$, DEPT) δ = 155.3 (C), 154.8 (C), 149.3 (CH), 137.9 (CH), 136.9 (CH), 135.9 (C), 121.1 (CH), 120.7 (CH), 68.7 (CH_2), 37.5 (CH_3), 30.5 (CH_2), 28.8 (CH_2).

Mesylate 11. (a) Directly from 8 and 9. A mixture of dimesylate **8** (0.71 g, 1.40 mmol), tris(*p*-*tert*-butylphenyl)(4-hydroxyphenyl)-methane **9** (0.71 g, 1.40 mmol), and K_2CO_3 (0.29 g, 2.1 mmol) in DMF (150 mL) was stirred at 75 °C under Ar for 18 h. Solvent was evaporated and the crude treated with CH_2Cl_2, washed with H_2O, dried over Na_2SO_4, and filtered. After removal of the solvent, a yellow solid was obtained, which was subjected to column chromatography on alumina (CH_2Cl_2 containing 0−1% MeOH) to afford a mixture of alcohol **10** and mesylate **11** in 46% yield. A second fast alumina column (CH_2Cl_2−0.5%) yielded pure alcohol **10** (0.374 g, 32%) and pure mesylate **11** (0.166 g, 13%), both as white solids. **10**: ^{1}H NMR (200 MHz, $CDCl_3$) δ = 8.56−8.51 (m, 4H), 8.40 (d, J = 7.8 Hz, 2H), 7.93 (t, J = 7.8 Hz, 1H), 7.74−7.66 (m, 2H), 7.24 (d, J = 8.8 Hz, 6H), 7.09 (d, J = 8.8 Hz, 8H), 6.78 (d, J = 8.9 Hz, 2H), 3.99 (t, J = 6.0 Hz, 2H), 3.74 (t, J = 6.3 Hz, 2H), 2.95−2.77 (m, 4H), 2.20−2.11 (m, 2H), 2.03−1.89 (m, 2H), 1.60 (br s, 1H), 1.30 (s, 27H); FAB-MS *m*/*z* (relative intensity) 836.3 (100, MH^+), 702.2 (9, $[M - (t\text{-}BuC_6H_4)]^+$), 411.1 (24, $[(t\text{-}BuC_6H_4)_3C]^+$). **11**: ^{1}H NMR (200 MHz, $CDCl_3$) δ = 8.58−8.51 (m, 4H), 8.41 (d, J = 8.1 Hz, 2H), 7.94 (t, J = 7.8 Hz, 1H), 7.74−7.67 (m, 2H), 7.24 (d, J = 8.9 Hz, 6H), 7.09 (d, J = 8.9 Hz, 8H), 6.78 (d, J = 8.9 Hz, 2H), 4.29 (t, J = 6.2 Hz, 2H), 3.99 (t, J = 6.0 Hz, 2H), 3.03 (s, 3H), 2.95−2.82 (m, 4H), 2.22−2.08 (m, 4H), 1.30 (s, 27H); FAB-MS *m*/*z* (relative intensity) 914.5 (100, MH^+), 780.4 (14, $[M - (t\text{-}BuC_6H_4)]^+$), 411.3 (53, $[(t\text{-}BuC_6H_4)_3C]^+$).

(b) Via Alcohol 10. Mesyl chloride (0.31 mL, 4.0 mmol) in anhydrous CH_2Cl_2 (10 mL) was added dropwise over a stirred solution of **10** (0.84 g, 1.0 mmol) and freshly distilled NEt_3 (0.84 mL, 6.0 mmol) in anhydrous CH_2Cl_2 (30 mL) at −3 °C, and the mixture was stirred at −2 °C for 4 h. The reaction mixture was washed with cold H_2O, dried over Na_2SO_4, and filtered. Removal of the solvent led to a white solid (0.91 g, 100%). TLC (alumina; CH_2Cl_2−1% MeOH) showed one spot, and the product was used in the next step without further purification.

Bromo Derivative 12. A mixture of crude mesylate **11** (0.91 g) and anhydrous LiBr (0.434 g, 5.0 mmol) in acetone (30 mL) was refluxed under Ar for 2 h. Solvent was evaporated, and the residue was taken in CH_2Cl_2, washed with cold H_2O, dried over Na_2SO_4, and filtered. Solvent was removed, and the crude was filtered through a short alumina column (CH_2Cl_2) to yield pure **12** as a white solid (0.72 g, 80% yield from alcohol **10**): ^{1}H NMR (200 MHz, $CDCl_3$) δ = 8.57−8.51 (m, 4H), 8.40 (d, J = 7.8 Hz, 2H), 7.94 (t, J = 7.8 Hz, 1H), 7.74−7.67 (m, 2H), 7.24 (d, J = 8.9 Hz, 6H), 7.09 (d, J = 8.9 Hz, 8H), 6.78 (d, J = 8.9 Hz, 2H), 3.99 (t, J = 6.0 Hz, 2H), 3.44 (t, J = 6.4 Hz, 2H), 2.95−2.85 (m, 4H), 2.30−2.10 (m, 4H), 1.30 (s, 27H); FAB-MS *m*/*z* (relative intensity) 900.5 (100, MH^+), 818.5 (13, $[M - Br]^+$), 766.4 (11, $[M - (t\text{-}BuC_6H_4)]^+$), 411.3 (47, $[(t\text{-}BuC_6H_4)_3C]^+$).

Ligand 15. A titrated commercial solution of LDA in THF (ca. 1.5 M, 0.72 mL, 1.08 mmol) was slowly added dropwise to a degassed solution of 2-methyl-9-(*p*-anisyl)-1,10-phenanthroline **13** (0.31 g, 1.03 mmol) in anhydrous THF (20 mL) at −78 °C. The resulting deep purple solution was stirred under Ar at −78 °C for 2 h and then for 1 h from −78 to 0 °C. The mixture was cooled again to −78 °C, and a degassed solution of **12** (0.78 g, 0.86 mmol) in anhydrous THF (25 mL) was added dropwise. The resulting deep purple mixture was left at 0 °C and slowly allowed to reach room temperature during 16 h. The reaction mixture was then hydrolyzed at 0 °C with H_2O (20 mL). THF was removed, and the residue was taken in CH_2Cl_2, washed with H_2O, dried over Na_2SO_4, and filtered. Solvent was evaporated, and the residue was subjected to column chromatography on alumina (hexane−CH_2Cl_2) to yield **15** as a yellow solid (0.587 g, 61%): ^{1}H NMR (200 MHz, $CDCl_3$) δ = 8.57−8.48 (m, 4H), 8.40−8.34 (m, 4H), 8.26 (d, J = 8.5 Hz, 1H), 8.15 (d, J = 8.2 Hz, 1H), 8.06 (d, J = 8.5 Hz, 1H), 7.92 (t, J = 7.9 Hz, 1H), 7.74−7.67 (m, 4H), 7.51 (d, J = 8.2 Hz, 1H), 7.24 (d, J = 8.7 Hz, 6H), 7.11−7.05 (m, 10H), 6.78 (d, J = 8.9 Hz, 2H), 3.99 (t, J = 6.0 Hz, 2H), 3.88 (s, 3H), 3.29 (t, J = 7.6 Hz, 2H), 2.95−2.81 (m, 4H), 2.21−2.07 (m, 4H), 2.00−1.88 (m, 2H), 1.30 (s, 27H); FAB-MS *m*/*z* (relative intensity) 1118.6 (100, MH^+; calcd 1118.6), 818.5 (13, $[M - C_{20}H_{15}N_2O]^+$), 411.3 (71, $[(t\text{-}BuC_6H_4)_3C]^+$), 300.1 (83, $[C_{20}H_{16}N_2O]^+$).

Ligand 16. A solution of **15** (0.28 g, 0.25 mmol) in dry DMF (13 mL) was added to EtSNa (0.105 g, 1.25 mmol), and the mixture was stirred at 110 °C under a slow flow of Ar for 16 h. The solution was allowed to reach 60 °C, and 15 mL of H_2O was added. The mixture was stirred at 60 °C for 20 min, poured into H_2O (30 mL), and extracted with CH_2Cl_2. The organic phase was separated, and the aqueous phase was treated with solid NH_4Cl and extracted again with more CH_2Cl_2. The combined organic layers were washed with buffered aqueous solution (pH = 7) and then with water, dried over Na_2SO_4, and filtered.

Evaporation of the solvent led to a brown solid, which was purified by column chromatography on alumina (CH_2Cl_2-2% MeOH) to yield a yellow solid (0.222 g, 80%): ^{1}H NMR (200 MHz, $CDCl_3$) δ = 8.55 (d, $J \approx 2$ Hz, 1H), 8.51 (d, $J \approx 2$ Hz, 1H), 8.44 (d, J = 8.1 Hz, 1H), 8.43 (d, J = 8.1 Hz, 1H), 8.36−8.31 (m, 2H), 8.18−8.13 (m, 2H), 8.05 (d, J = 8.7 Hz, 2H), 7.93−7.84 (m, 2H), 7.69 (s, 2H), 7.69−7.62 (m, 2H), 7.50 (d, J = 8.2 Hz, 1H), 7.23 (d, J = 8.6 Hz, 6H), 7.11−7.05 (m, 8H), 6.92 (d, J = 8.7 Hz, 2H), 6.77 (d, J = 8.9 Hz, 2H), 3.97 (t, J = 6.0 Hz, 2H), 3.27 (t, J = 7.4 Hz, 2H), 2.91−2.74 (m, 4H), 2.21−1.85 (m, 6H), 1.30 (s, 27H); FAB-MS *m*/*z* (relative intensity) 1104.8 (52, MH^+; calcd 1104.6), 818.6 (7, $[M - C_{19}H_{13}N_2O]^+$), 411.4 (48, $[(t\text{-}BuC_6H_4)_3C]^+$), 286.2 (100, $C_{19}H_{14}N_2O^+$).

Semirotaxane 19·PF$_6$. A solution of $Cu(MeCN)_4PF_6$ (19.6 mg, 0.053 mmol) in degassed MeCN (9 mL) was transferred via a cannula to a stirred solution of **17** (28.3 mg, 0.050 mmol) in CH_2Cl_2 (9 mL), all under an atmosphere of Ar. The resulting orange solution was stirred at room temperature for 30 min. Then it was added via a cannula to a degassed solution of **15** (56 mg, 0.050 mmol) in CH_2Cl_2 (20 mL), and the resulting brown red solution was stirred under Ar at room temperature for 16 h. Solvent was evaporated and the residue filtered through a short alumina column (CH_2Cl_2−0.5% MeOH) to give **19·PF$_6$** as a brown-red solid (76 mg, 80%): ^{1}H NMR (400 MHz, CD_2Cl_2) δ = 8.68 (d, J = 8.3 Hz, 1H), 8.57 (br s, 1H), 8.49−8.45 (m, 4H), 8.40 (d, J = 7.5 Hz, 1H), 8.29 (d, J = 8.8 Hz, 1H), 8.24 (d, J = 7.8 Hz, 1H), 8.23 (d, J = 7.8 Hz, 1H), 8.10 (br s, 1H), 8.06 (d, J = 8.8 Hz, 1H), 8.00 (s, 2H), 7.92 (d, J = 8.3 Hz, 2H), 7.89 (t, J = 7.8 Hz, 1H), 7.76−7.73 (m, 2H), 7.58 (d, J = 8.3 Hz, 1H), 7.33 (d, J = 8.7 Hz, 4H), 7.29−7.14 (m, 17H), 6.81 (d, J = 9.0 Hz, 2H), 5.97 (d, J = 8.7 Hz, 4H), 5.90 (d, J = 8.6 Hz, 2H), 4.02 (t, J = 6.2 Hz, 2H), 3.81 (s, 4H), 3.70−3.66 (m, 4H), 3.57−3.52 (m, 8H), 3.46 (s, 3H), 3.46−3.43 (m, 4H), 2.93−2.89 (m, 2H), 2.53−2.49 (m, 2H), 2.28 (t, J = 7.2 Hz, 2H), 2.19−2.12 (m, 2H), 1.56−1.50 (m, 2H), 1.30 (s, 27H), 1.32−1.26 (m, 2H); UV−vis (MeCN) λ_{max} = 442 nm (ϵ = 3100); FAB-MS *m*/*z* (relative intensity) 1747.8 (21, $[M - PF_6]^+$; calcd 1747.8), 1180.5 (90, $[M - \mathbf{17} - PF_6]^+$), 629.2 (80, $[Cu(\mathbf{17})]^+$), 411.3 (100, $[(t\text{-}BuC_6H_4)_3C]^+$).

Threaded Precursor 20$^+$. A solution of $Cu(MeCN)_4PF_6$ (37.3 mg, 0.100 mmol) in degassed MeCN (10 mL) was transferred via a cannula to a stirred solution of macrocycle **17** (56.7 mg, 0.100 mmol) in CH_2Cl_2 (10 mL) under Ar, and the resulting orange solution was stirred at room temperature for 20 min. Then, a degassed solution of **16** (110 mg, 0.100 mmol) in CH_2Cl_2 (20 mL) was transferred via a cannula, resulting in the immediate formation of a brown-red solution, which was stirred under Ar at room temperature for 14 h. Solvent was evaporated to give a brown-red solid (188 mg, 100%), which was pure enough to be used in the following step without further purification: ^{1}H NMR (200 MHz, CD_2Cl_2) δ = 8.67 (d, J = 8.3 Hz, 1H), 8.56 (br s, 1H), 8.51−8.37 (m, 5H), 8.30−8.20 (m, 3H), 8.11 (br s, 1H), 8.06−7.70 (m, 8H), 7.57 (d, J = 8.3 Hz, 1H), 7.33−7.14 (m, 19H), 7.04 (d, J = 8.6 Hz, 2H), 6.80 (d, J = 9.0 Hz, 2H), 5.94 (d, J = 8.6 Hz, 4H), 5.86 (d, J = 8.6 Hz, 2H), 4.01 (t, $J \approx 6$ Hz, 2H), 3.80 (br s, 4H), 3.70−3.65 (m, 4H), 3.58−3.51 (m, 8H), 3.46−3.41 (m, 4H), 2.94−2.86 (m, 2H), 2.54−2.42 (m, 2H), 2.32−2.24 (m, 2H), 2.18−2.10 (m, 2H), 1.60−1.50 (m, 2H), 1.30 (s, 27H), 1.34−1.24 (m, 2H).

2-Hydroxyethyl *p*-[Tris(*p*-*tert*-butylphenyl)methyl]phenyl Ether (21). A mixture of phenol **9** (0.51 g, 1.0 mmol), THP-protected bromoethanol (0.23 g, 1.1 mmol), and K_2CO_3 (0.17 g, 1.2 mmol) in DMF (40 mL) was stirred under Ar at 65 °C for 18 h. DMF was evaporated and the residue taken in CH_2Cl_2, washed with brine, dried over Na_2SO_4, and filtered. Evaporation of the solvent followed by column chromatography on silica gel (hexanes−ether) led to the corresponding THP-protected alcohol as a white solid (0.46 g). This solid was refluxed in EtOH, in the presence of a catalytic amount of concentrated HCl, for 16 h. The mixture was neutralized with some drops of concentrated NaOH. Solvent was rotary evaporated, and the residue was dissolved in CH_2Cl_2, washed with brine, dried over Na_2SO_4, and filtered. After evaporation of the solvent and column chromatography on silica gel (hexanes−ether), alcohol **21** was obtained as a white solid (0.31 g, 56%): ^{1}H NMR (200 MHz, $CDCl_3$) δ = 7.24 (d, J = 8.8 Hz, 6H), 7.10 (d, J = 9.0 Hz, 2H), 7.08 (d, J = 8.8 Hz, 6H), 6.79 (d, J = 9.0 Hz, 2H), 4.09−4.05 (m, 2H), 3.98−3.91 (m, 2H), 2.00 (t, J = 6.2 Hz, 1H), 1.30 (s, 27H); FAB-MS *m*/*z* (relative intensity) 548.1 (33, M^+; calcd 548.4), 415.1 (100, $[M - (t\text{-}BuC_6H_4)]^+$), 411.3 (74, $[(t\text{-}BuC_6H_4)_3C]^+$).

2-Methanosulfonylethyl *p*-[Tris(*p*-*tert*-butylphenyl)methyl]phenyl Ether (22). Mesyl chloride (0.06 mL, 0.77 mmol) in anhydrous CH_2Cl_2 (2.5 mL) was slowly added dropwise over a stirred solution of **21** (0.105 g, 0.19 mmol) and freshly distilled NEt_3 (0.10 mL, 0.73 mmol) in anhydrous CH_2Cl_2 (6 mL) at −3 °C. The mixture was stirred under Ar at −2 °C for 3.5 h. The solution was then washed with cold water, dried over Na_2SO_4, and filtered. Solvent was evaporated, and the resulting crude was filtered through a short alumina column (CH_2Cl_2 as eluent), to afford **22** as a white solid (0.116 g, 97%): ^{1}H NMR (200 MHz, $CDCl_3$) δ = 7.24 (d, J = 8.7 Hz, 6H), 7.12 (d, J = 9.0 Hz, 2H), 7.07 (d, J = 8.7 Hz, 6H), 6.77 (d, J = 9.0 Hz, 2H), 4.59−4.54 (m, 2H), 4.25−4.20 (m, 2H), 3.09 (s, 3H), 1.30 (s, 27H); FAB-MS *m*/*z* (relative intensity) 626.5 (20, M^+; calcd 626.3), 493.4 (100, $[M - (t\text{-}BuC_6H_4)]^+$), 411.5 (67, $[(t\text{-}BuC_6H_4)_3C]^+$).

2-Bromoethyl *p*-[Tris(*p*-*tert*-butylphenyl)methyl]phenyl Ether (23). A mixture of **22** (0.116 g, 0.185 mmol) and anhydrous LiBr (0.079 g, 0.91 mmol) in acetone (6 mL) was refluxed under Ar for 2 h. Solvent was evaporated, and the residue was taken in CH_2Cl_2, washed with water, and dried over Na_2SO_4. After filtration and evaporation of the solvent, a white-yellow solid was obtained (0.112 g, 100%). TLC (alumina; CH_2Cl_2) showed only one pot, and the product was used in the following step without further purification: ^{1}H NMR (200 MHz, $CDCl_3$) δ = 7.24 (d, J = 8.7 Hz, 6H), 7.10 (d, J = 8.9 Hz, 2H), 7.07 (d, J = 8.7 Hz, 6H), 6.78 (d, J = 8.9 Hz, 2H), 4.27 (t, J = 6.3 Hz, 2H), 3.63 (t, J = 6.3 Hz, 2H), 1.30 (s, 27H).

Rotaxane 24$^+$. Cs_2CO_3 (65 mg, 0.20 mmol) in degassed DMF (10 mL) was transferred via a cannula, during a 1-h period, to an argon-flushed solution of crude threaded complex **20**$^+$ (188 mg), bromoalkyl derivative **23** (73 mg, 0.120 mmol), and ascorbic acid (4.4 mg, 0.025 mmol) in DMF (20 mL) at 45 °C. Once the addition was finished, the mixture was stirred under Ar at 55 °C for 18 h and then at 65 °C for 6 h more. DMF was evaporated and the resulting crude taken in CH_2Cl_2 and washed with H_2O. The organic solution was vigorously stirred with excess of a KPF_6-saturated aqueous solution at room temperature for 4 h and then washed again with H_2O. After evaporation of the solvent and two successive column chromatographies on alumina (CH_2Cl_2 containing 0−0.2% MeOH), rotaxane **24·PF$_6$** was obtained as a brown-red solid (88 mg, 40%): ^{1}H NMR (400 MHz, CD_2Cl_2) δ = 8.70 (d, J = 8.3 Hz, 1H), 8.56 (br s, 1H), 8.48−8.46 (m, 2H), 8.41−8.36 (m, 3H), 8.29 (d, J = 8.9 Hz, 1H), 8.24 (br d, $J \approx 7.8$ Hz, 2H), 8.12 (br s, 1H), 8.05 (d, J = 8.9 Hz, 1H), 7.89−7.85 (m, 5H), 7.76−7.71 (m, 2H), 7.59 (d, J = 8.3 Hz, 1H), 7.33 (d, J = 8.7 Hz, 4H), 7.32−7.15 (m, 29H), 7.11 (d, J = 8.6 Hz, 2H), 6.92 (d, J = 9.0 Hz, 2H), 6.79 (d, J = 9.0 Hz, 2H), 5.97 (d, J = 8.7 Hz, 4H), 5.92 (d, J = 8.6 Hz, 2H), 4.26−4.24 (m, 2H), 4.00 (t, J = 6.0 Hz, 2H), 3.89−3.87 (m, 2H), 3.80 (br s, 4H), 3.70−3.67 (m, 4H), 3.58−3.54 (m, 8H), 3.46−3.43 (m, 4H), 2.91−2.87 (m, 2H), 2.53−2.49 (m, 2H), 2.33−2.29 (m, 2H), 2.18−2.12 (m, 2H), 1.60−1.54 (m, 2H), 1.30 (s, 27H), 1.29 (s, 27H), 1.34−1.26 (m, 2H); UV−vis (MeCN) λ_{max} = 442 nm (ϵ = 2700); FAB-MS *m*/*z* 2265.2 ($[M - PF_6]^+$; calcd 2265.1), 1698.0 ($[M - \mathbf{17} - PF_6]^+$), 629.2 ($[Cu(\mathbf{17})]^+$).

Demetalated Rotaxane 25. A solution of KCN (0.117 g, 1.80 mmol) in H_2O (2 mL) was added to a stirred brown-red solution of rotaxane **24**$^+$ (82 mg, 0.034 mmol) in CH_2Cl_2−MeCN (2:3, 10 mL). The resulting mixture was vigorously stirred at room temperature for 1 h (the red color characteristic of the Cu(I) complex disappeared in about 5−10 min). Solvent was evaporated, and the residue was taken in CH_2Cl_2, washed with H_2O, and dried over Na_2SO_4. After filtration and evaporation of the solvent, there was obtained a white-yellow solid (0.075 g), which was purified by column chromatography on alumina (CH_2Cl_2 containing 0−0.5% MeOH) to afford a white solid (63 mg, 84%): ^{1}H NMR (400 MHz, CD_2Cl_2) δ = 8.50−8.45 (m, 4H), 8.37−8.28 (m, 8H), 8.20 (d, J = 8.4 Hz, 2H), 8.18 (d, J = 8.6 Hz, 1H), 8.14 (d, J = 8.2 Hz, 1H), 8.00 (d, J = 8.6 Hz, 1H), 7.96 (d, J = 8.4 Hz, 2H), 7.87 (t, J = 7.9 Hz, 1H), 7.72 (s, 2H), 7.71 (s, 2H), 7.60 (dd, J = 7.9 and 2.3 Hz, 1H), 7.58 (dd, J = 7.9 and 2.3 Hz, 1H), 7.49 (d, J = 8.2 Hz, 1H), 7.25−7.06 (m, 30H), 6.92−6.86 (m, 8H), 4.44−4.42 (m, 2H), 4.36−4.34 (m, 2H), 4.02−3.95 (m, 6H), 3.62−3.46 (m, 16H),

3.19 (t, $J = 7.7$ Hz, 2H), 2.81 (t, $J = 7.7$ Hz, 2H), 2.73 (t, $J = 7.6$ Hz, 2H), 2.14−2.06 (m, 2H), 2.03−1.95 (m, 2H), 1.84−1.77 (m, 2H), 1.29 (s, 27H), 1.27 (s, 27H); FAB-MS *m*/*z* (relative intensity) 220.1 (75, $[MH_2]^+$, calcd 2202), 1635.9 (80, $[MH_2 - \mathbf{17}]^+$, calcd 1635), 567.3 (100, $[\mathbf{17}H]^+$, calcd 567).

Acknowledgment. This research was supported by the CNRS (France), Italian CNR, University of Bologna (Progetto Mareriali Innovativi), MURST (Progetto Dispositivi Supramoleclari), and EC HCM network ERB CHR XCT 940492 "Transition Metals in Supramolecular catalysis". We thank M. Minghetti for technical assistance. P.G. thanks the *Ministerio de Educacion y Ciencia* (Spain) for postdoctoral fellowship support.

JA984051W